Chance and contingency in B cell evolution limit the similarity of antibody responses to infection across individuals

Marcos C. Vieira[1*], Anna-Karin E. Palm[2], Christopher T. Stamper[3,4], Micah E. Tepora[2], Khoa D. Nguyen[5], Tho D. Pham[5], Scott D. Boyd[5], Patrick C. Wilson[2,6], Sarah Cobey[1*]

***For correspondence:**
mvieira@uchicago.edu (MCV);
cobey@uchicago.edu (SC)

[1]Department of Ecology and Evolution, University of Chicago, Chicago, USA; [2]Department of Medicine, Section of Rheumatology, University of Chicago, Chicago, USA; [3]Center for Infectious Medicine, Department of Medicine Huddinge, Karolinska Institutet, Karolinska University Hospital Huddinge, Stockholm, Sweden; [4]Committee on Immunology, University of Chicago, Chicago, USA; [5]Department of Pathology, Stanford University School of Medicine, Stanford, USA; [6]Gale and Ira Drukier Institute for Children's Health, Weill Cornell Medicine, New York City, USA

Abstract Antibody responses emerge from the competition of B cell lineages with different antigen receptors, each produced by the recombination of germline immunoglobulin genes. Which lineages win out can depend on subsequent somatic mutations that improve antigen binding, yet lineages using specific germline alleles can have higher affinity than others from the start or a higher propensity to adapt. How much do those germline-encoded advantages determine the outcome of B cell competition, potentially leading to predictable allele frequencies and sequence motifs in the response to the same antigen in different individuals? In simulations, we show that selection for receptors with germline-encoded specificity can lead to similar germline allele frequencies between individuals early in the response. As B cell lineages evolve, those early advantages are often overcome by lineages using different germline alleles in different individuals, leading to increasingly contingent patterns of germline allele usage over time. Consistent with simulations, mice experimentally infected with influenza virus have increasingly dissimilar germline allele frequencies and do not converge on similar CDR3 sequences or similar somatic mutations. These results suggest germline-encoded specificities might be selected to enable fast recognition of specific antigens early in the response, while diverse evolutionary routes to high affinity limit the predictability of responses to infection and vaccination in the long term.

Introduction

Antibodies owe their diversity and potency to evolution on two different timescales. B cell receptors, the precursors of secreted antibodies, are encoded by immunoglobulin genes diversified over hundreds of millions of years (***Marchalonis et al., 1998***; ***Flajnik, 2002***; ***Das et al., 2008***). Recombination of separate sets of genes encoding the receptor's heavy and light chains, combined with

insertions and deletions at the alleles' junctions, produces a unique receptor in each maturing B cell (***Hozumi and Tonegawa, 1976***; ***Brack et al., 1978***; ***Jackson et al., 2013***). The result is a diverse repertoire of naive (antigen-inexperienced) B cells collectively capable of binding virtually any antigen. Once activated, naive B cells expand into lineages that compete with each other for access to antigen and can undergo selection for somatic mutations that improve binding (***Eisen and Siskind, 1964***; ***Jacob et al., 1991***; ***Victora and Nussenzweig, 2012***). How much the various lineages grow, what antigens and epitopes they target and how well they do so determine the ultimate specificity and potency of the antibody repertoire.

A central question in the study of adaptive immunity is how much these outcomes depend on the initial set of germline immunoglobulin genes versus the subsequent evolution of fully-formed B cell receptors. Affinity maturation can vastly improve binding (***Liao et al., 2013***; ***McCarthy et al., 2019***), yet high affinity for particular epitopes can be "hardcoded" on individual germline alleles from the start. These germline-encoded specificities might arise as evolutionary spandrels — byproducts of immunoglobulin gene diversification — (***Gould and Lewontin, 1979***; ***Sangesland and Lingwood, 2021***), but they could be subsequently selected. For instance, germline alleles with innately high affinity for bacterial antigens might arise from long-term selection in vertebrate populations to recognize commonly encountered pathogens and commensals via broad classes of epitopes shared by these organisms (***Yeung et al., 2016***; ***Collins and Jackson, 2018***; ***Sangesland et al., 2020***).

Three lines of evidence support the idea that specific germline immunoglobulin alleles are better than others at binding particular antigens. First, structural characterization of individual antibodies shows that some variable (V) alleles can bind specific epitopes through germline-encoded motifs in complementarity-determining regions (CDRs) 1 and 2 (e.g., ***West et al. 2012***; ***Pappas et al. 2014***; ***Yeung et al. 2016***; ***Yuan et al. 2020***; ***Voss et al. 2021***). These antigen-binding regions are encoded solely by the receptor's V allele, whereas CDR3 spans the junction of V alleles with joining (J) and, in the case of the heavy chain, diversity (D) alleles. While epistatic interactions with other alleles might be important, germline-encoded motifs in CDRs1-2 could make specific V alleles more likely than others to bind specific antigens. A second line of evidence comes from experiments with transgenic mouse strains that each have a single heavy-chain V allele but multiple alleles in the other sets. Strains with specific V alleles have higher antibody titers against specific antigens than the other strains (***Sangesland et al., 2019***, ***2020***). A third line of evidence comes from sequencing studies, which often show that specific alleles, allele combinations or CDR3 sequences are overrepresented in the response to particular epitopes (reviewed by ***Dunand and Wilson 2015*** and ***Sangesland and Lingwood 2021***). Overrepresentation of specific alleles is often interpreted as a consequence of, and as indirect evidence for, the kind of germline-encoded specificity revealed by structural analyses or transgenic mouse experiments. In addition to different propensities to encode receptors with high affinity, overrepresentation of particular alleles might also reflect different potentials for subsequent adaptation during affinity maturation.

Yet the degree to which specific germline alleles are consistently overrepresented in individuals exposed to the same antigen varies widely for reasons that are poorly understood. In some cases, only a few germline alleles are represented in the response (e.g., ***Crews et al. 1981***; ***Cumano and Rajewsky 1985***, 1986; ***Guthmiller et al. 2021***, 2022), suggesting that germline-encoded specificities strongly predict the outcome of B cell competition and lead to highly similar repertoires. In other cases, most germline alleles are used (e.g. ***Di Niro et al. 2015***; ***Kuraoka et al. 2016***; ***Nielsen et al. 2020***; ***Robbiani et al. 2020***; ***Sakharkar et al. 2021***), only some of which appear overrepresented with respect to controls, suggesting that initial advantages of B cells with specific germline alleles do not strongly predict the outcome of B cell evolution and competition. Those studies vary not only in the complexity of the antigen and the type of B cell studied, but also in the amount of time since the exposure and thus the extent of affinity maturation. How the overrepresentation of specific alleles and the degree of similarity between individuals changes during the course of the response has not been systematically investigated.

Using simulations and experiments, we show that stochasticity and contingency in B cell evolution and competition counterbalance initial selection for receptors with specific germline alleles. Germline alleles can give B cell lineages an advantage over others early in the response, but which lineages ultimately dominate also depends on factors that are largely random with respect to the choice of germline allele, such as the occurrence and timing of mutations in different lineages. In simulations, these factors tend to produce increasingly contingent patterns of allele usage during the course of the response. We find patterns consistent with those dynamics in the B cell response of mice experimentally infected with influenza virus. Specific heavy-chain V alleles are consistently abundant in the repertoires of different infected mice early on, but allele usage becomes less consistent over time as large mutated lineages come to dominate the repertoire. Those dominant lineages use different germline V alleles in different mice, and lineages sharing the same allele rarely evolve the same somatic mutations. These results suggest that germline-encoded specificities and those evolved later by affinity maturation are important at different phases of the response. Selection to reinforce germline-encoded specificities in the long-term evolution of jawed vertebrates might be driven by the fitness benefits of responding rapidly to commonly encountered pathogens. The lack of consistency in germline allele usage or specific mutations later in the response also suggests no pronounced differences in the adaptability of different immunoglobulin genes.

Results

We begin by asking what factors might affect germline allele frequencies in the B cell response, before turning to a mathematical model to understand how those factors interact. By response we mean the set of B cell populations that bind a specific epitope, antigen or pathogen: germinal center cells, memory cells and short- and long-lived plasma cells. Since all those populations descend from naive B cells, germline allele frequencies in the response depend partly on allele frequencies in the naive repertoire, which vary widely between alleles but tend to be positively correlated between individuals (although heritable variation exists; ***Glanville et al. 2011***; ***Watson et al. 2017***; ***Collins et al. 2020***). Here, we focus on factors that cause some alleles to be over or underrepresented in the response relative to their baseline frequency in naive B cells. How much a germline allele increases or decreases in frequency depends on how many naive B cells using that allele are activated, and how much they divide inside or outside germinal centers, relative to naive cells using other alleles. Within specific cell types, germline allele frequencies also reflect how often cells using each allele differentiate into each cell type. We start by focusing on germline allele frequencies in the response as a whole, across cell types.

There are two non-mutually exclusive reasons why the total number and size of B cell lineages involved in the response might vary between germline immunoglobulin alleles (***Figure 1***). The first is if using particular germline alleles tends to give B cell lineages an advantage over others. This advantage could be a higher initial affinity, a greater capacity to evolve high affinity during affinity maturation, or both:

> *Germline-encoded affinity.* Since affinity is a property of the entire recombined receptor, not of its individual constituent alleles, naive B cells using a particular germline allele have a distribution of possible affinities depending on the choice of alleles from the other sets in the heavy and light chains (including insertions and deletions at the alleles' junctions). If individuals have similar sets of germline alleles at similar frequencies in the naive repertoire, and if the probabilities of different allele combinations are similar, then the affinity distribution for any given germline allele will be similar in different individuals. Yet different germline alleles might have different affinity distributions, leading to different fitness distributions for naive B cells using each allele. For instance, naive B cells using a specific heavy-chain V allele might bind the antigen well across all combinations with other alleles via CDRs1-2 (***Figure 1***, orange allele), while naive B cells using a different V allele may bind poorly across the board (***Figure 1***, purple allele) or have low affinity overall but high affinity in certain combinations (***Figure 1***,

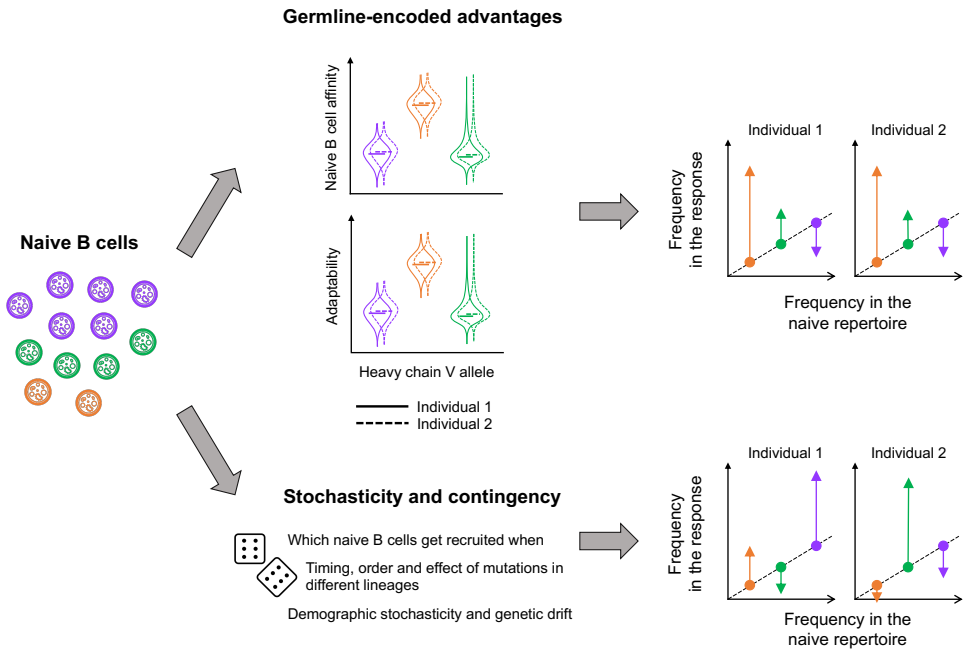

Figure 1. Schematic of factors controlling germline allele frequencies in the B cell response to a particular antigen. Three heavy-chain V alleles (orange, purple and green) are present at different frequencies in naive B cells. Although they have the same heavy-chain V allele, naive cells of the same color can have different alleles from the other sets in the heavy and light chains (and different insertions and deletions at the alleles' junctions). Different combinations produce receptors with different affinities for the antigen and different propensities for adaptation during affinity maturation. If these distributions vary between heavy-chain V alleles, alleles more likely to produce receptors with high affinity or high adaptability will tend to increase in frequency relative to the naive repertoire. These deviations are expected to be consistent in individuals sharing similar sets of germline alleles at similar frequencies in the naive repertoire. However, which B cell lineages dominate the response – and what heavy-chain V alleles they happen to use – is also contingent on events that are largely unpredictable, potentially leading to uncorrelated frequency deviations in the response of different individuals.

green allele).

Germline-encoded adaptability. Like initial affinity for a particular antigen, the potential for a B cell receptor to evolve higher affinity is a property of the entire receptor, not of individual germline alleles. Yet receptors using different alleles might have different propensities to adapt (***Figure 1***), for instance if they tend to have different rates of beneficial and deleterious mutations. Variation in mutability occurs because the enzymes responsible for mutating the B cell receptor target different nucleotide motifs at different rates (***Rogozin and Kolchanov, 1992***; ***Rogozin and Diaz, 2004***; ***Yaari et al., 2013***; ***Wei et al., 2015***), so variation in the motif composition of germline immunoglobulin alleles can lead to differences in the frequency and distribution of mutations. Variation in the relative probabilities of beneficial and deleterious mutations arises from epistasis: mutations are more likely to change affinity or disrupt the receptor's function in some backgrounds than in others (***Boyer et al., 2016***; ***Schulz et al., 2021***).

A second reason why specific germline alleles might become over or underrepresented is the role of chance and contingency in B cell activation, evolution and competition. Contingency means that although these processes are not random (since they are shaped by selection for affinity), their precise outcome depends on the occurrence, order and timing of events that are largely unpredictable (***Gould, 1989***; ***Beatty and Carrera, 2011***; ***Blount et al., 2018***). Which lineages come to dom-

Table 1. Default parameter values used in simulations.

Parameter	Symbol	Value
Baseline average naive B cell affinity	a	1
Baseline standard deviation of naive B cell affinity	σ	1
Expected number of lineages seeding each GC	I_{total}	200
GC carrying capacity	K	2000
Duration of GC immigration phase	t_{imm}	6 days
Maximum rate of cell division	μ_{max}	3 cell^{-1}day^{-1}
Death rate	δ	0.2 cell^{-1}day^{-1}
Standard deviation of mutation effect size	β	4

inate the response, and which germline alleles they use, will be contingent on how those events play out. Several sources of stochasticity in B cell dynamics could lead to contingent germline allele frequencies:

Stochasticity in B cell activation and in the colonization of germinal centers. Because the number of naive B cells is finite and the probabilities of different VDJ combinations vary by orders of magnitude (***Elhanati et al., 2015***), rare germline allele combinations with high affinity may be present in the naive repertoires of some individuals but not others. Even if present in most individuals, low-frequency, high-affinity germline-allele combinations might, simply by chance, be recruited only in some of them (for instance, if none of the rare naive cells come near the site of the response in a given individual).

Since germinal centers have a limited size, lineages that happen to arrive first might prevent others from establishing in the germinal center (similar to species competing for access to a site; ***Chase 2003***; ***Fukami 2015***). Whether such "priority effect" does occur in germinal centers is unknown.

Stochasticity in the timing, order and effect of mutations. Which lineages ultimately evolve the highest affinity and outcompete the others is contingent on the precise timing, order and effect of mutations in each lineage. For instance, the timing and effect of mutations affect the outcome of clonal interference – when multiple affinity-increasing mutations within a lineage or in different lineages compete for fixation (***Desai and Fisher, 2007***). Due to epistasis, the same B cell lineage could end up with very different affinities by acquiring mutations in different orders (***Starr and Thornton, 2016***).

Demographic stochasticity and genetic drift. Demographic stochasticity and genetic drift might be important, especially early in the response when population sizes are small. Demographic stochasticity might tip the balance of competition between lineages, driving some to extinction purely by chance. Genetic drift might cause new mutations to be fixed within a lineage even if they are neutral or deleterious or become extinct even if they are beneficial. The loss of newly arisen beneficial mutations due to drift is important even in large populations.

While both contingency and germline-encoded advantages can cause germline alleles to increase in frequency relative to the naive repertoire, only the latter are expected to produce consistent deviations in the response of different individuals exposed to the same antigen (provided individuals have similar sets of germline alleles) (***Figure 1***). The correlation in frequency deviations between individuals can therefore be used to measure how strongly germline-encoded advantages shape the outcome of B cell competition and evolution.

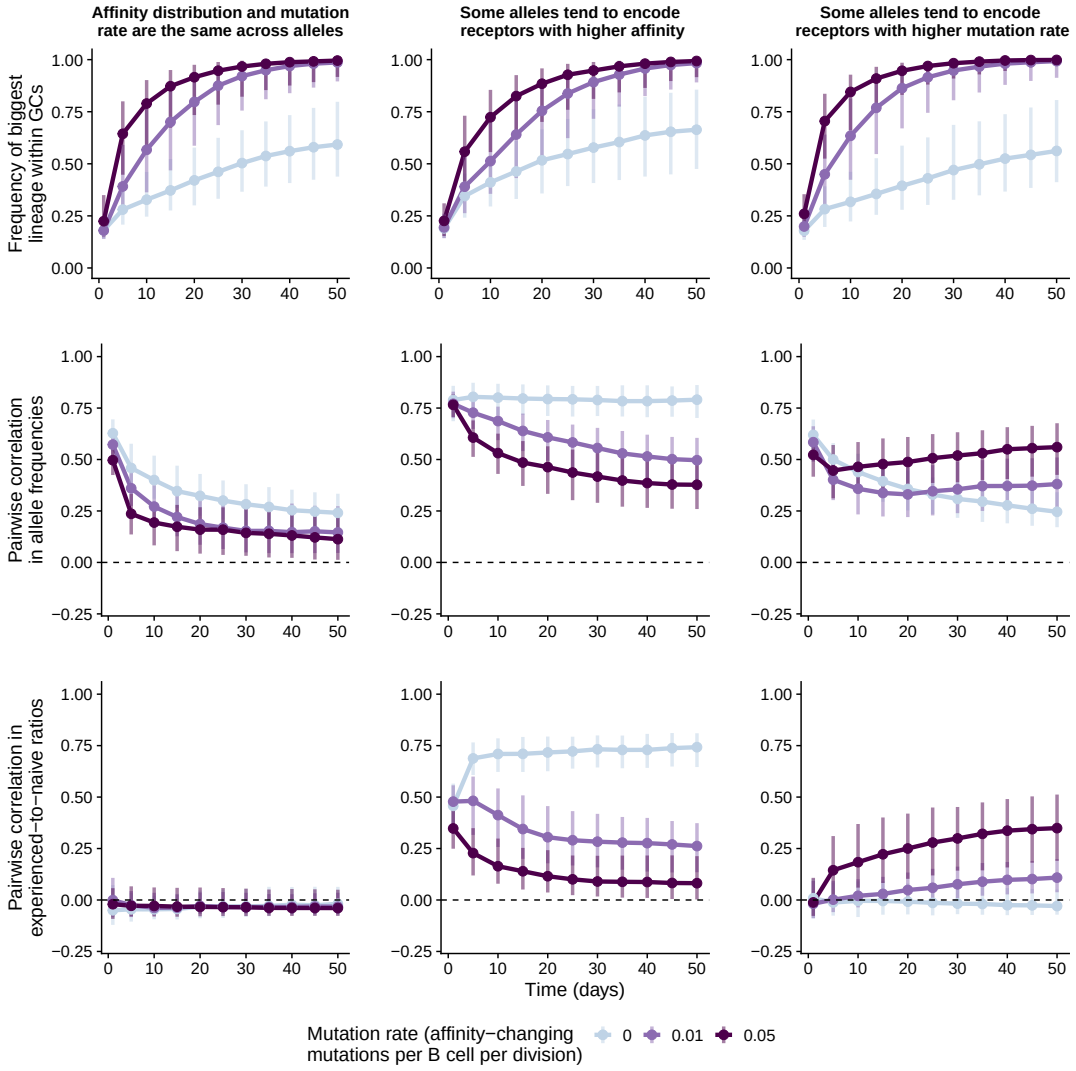

Figure 2. Evolution of allele frequencies in the B cell response simulated under different scenarios. For each scenario, we simulated 20 individuals, each with 15 germinal centers. We track the frequency of the biggest B cell lineage within each germinal center (top row) and between-individual correlations in allele frequencies (middle row) and in frequency deviations relative to the naive repertoire (bottom row). Points and vertical bars represent the median and the 1st and 4th quartiles, respectively. Values of parameters shared across scenarios are shown in Table 1. High-affinity alleles have naive affinity distributions with a mean increased by s = 1.5 relative to other alleles. High-mutation alleles have the baseline mutation rate multiplied by $\gamma = 6$.

Figure 2–Figure supplement 1. Simulations under the equivalent-alleles scenario.

Figure 2–Figure supplement 2. Simulations under the high-affinity scenario.

Figure 2–Figure supplement 3. Frequency of high-affinity alleles within simulated germinal centers.

Figure 2–Figure supplement 4. Simulations under high-mutability scenario.

Figure 2–Figure supplement 5. Combined frequency of high-mutability alleles.

Figure 2–Figure supplement 6. Sensitivity to the choice of correlation coefficient.

Similarity in germline allele frequencies reflects a balance between contingency and germline-encoded advantages

To understand how germline-encoded advantages interact with chance and contingency to shape the B cell repertoire, we used a stochastic mathematical model to simulate B cell evolution and competition in germinal centers (Methods: “Model of B cell dynamics”; Table 1). Rather than making quantitative predictions based on realistic parameter values, our goal was to investigate the

qualitative behavior of germline allele frequencies in the response and their deviations from the naive repertoire under different scenarios. The model focuses on the subset of the B cell response derived from germinal centers (the canonical sites of somatic hypermutation and B cell evolution), without considering extrafollicular B cell populations that expand outside of germinal centers (although reports of selection and somatic hypermutation in those populations suggest they might have similar dynamics; ***Di Niro et al. 2015***; ***Elsner and Shlomchik 2020***). To simulate selection for affinity, B cells are stochastically sampled to immigrate or divide based on their affinity relative to other cells in the naive repertoire (in the case of immigration) or in the germinal center (in the case of division). Dividing B cells then undergo affinity-changing mutations with some probability. To represent variation in germline-encoded affinity and adaptability, B cells using different heavy chain germline V alleles can have different naive affinity distributions. The variation within each distribution in turn represents the effects of stochasticity in VDJ recombination. The model also allows different germline V alleles to have different mutation rates, representing one aspect of variation in adaptability. We simulated 20 individuals, each with 15 germinal centers. We based these simulated individuals on mice for which we empirically estimated the set of heavy chain V alleles and their frequencies in the naive repertoire. These mice typically had about 75 heavy-chain V alleles (60-70 of which were typically shared between a pair of mice), and allele frequencies in the naive repertoire were strongly correlated between mice (***Figure 3***A-B).

If all germline alleles have the same naive affinity distribution and the same mutation rate, the model predicts that allele frequencies will be positively correlated between individuals early in the response but less so over time (***Figure 2***, left column; ***Figure 2–Figure Supplement 1***). The positive correlation early on arises from the correlation in naive allele frequencies between individuals: Assuming identical affinity distributions between germline alleles, the alleles tend to arrive in germinal centers in the same frequencies in which they occur in the naive repertoire. The subsequent decrease in allele-frequency correlations reflects the increasing role of stochasticity and contingency. Over time, due to selection, each germinal center tends to become dominated by the lineage with the highest affinity (***Figure 2***, left column, top row). With no differences in affinity or adaptability between germline alleles, which lineages ultimately evolve the highest affinity is completely random with respect to the choice of germline allele, and so allele-frequency correlations between individuals decrease while deviations from the naive repertoire (measured as the ratio between experienced and naive frequencies) remain uncorrelated throughout the response (***Figure 2***, left column, bottom row).

If some germline alleles tend to encode receptors with higher affinity than others, the model predicts that both allele frequencies and their deviations from the naive repertoire will be positively correlated between individuals early in the response, but chance and contingency reduce this correlation over time (***Figure 2***, middle column; ***Figure 2–Figure Supplement 2***). Without somatic hypermutation, both types of correlation remain high over time as germinal centers are consistently dominated by B cell lineages using high-affinity alleles (***Figure 2–Figure Supplement 3***). As the rate or the effect size of somatic hypermutation increases, so does the opportunity for B cell lineages using low-affinity alleles to overcome the initial advantage of those using high-affinity alleles (***Figure 2–Figure Supplement 3***). In the model, precisely which low-affinity alleles are used by lineages that do so is a matter of chance, since all B cells have the same probability of acquiring beneficial mutations irrespective of the germline V allele they use. As a result, both types of correlation between individuals decrease over time. In practice, due to different fitness landscapes between germline alleles, germline-encoded advantages might be preferentially overcome by lineages with specific alleles, allele combinations or heavy-light chain pairings.

Finally, when some germline alleles have a higher mutation rate than others, B cell lineages with high-mutation alleles are likely to dominate germinal centers in the long term due to their propensity to adapt (***Figure 2–Figure Supplement 5***), countering the tendency for allele frequencies to become less correlated over time and leading to a positive correlation in frequency deviations later in the response (***Figure 2***, right column; ***Figure 2–Figure Supplement 4***).

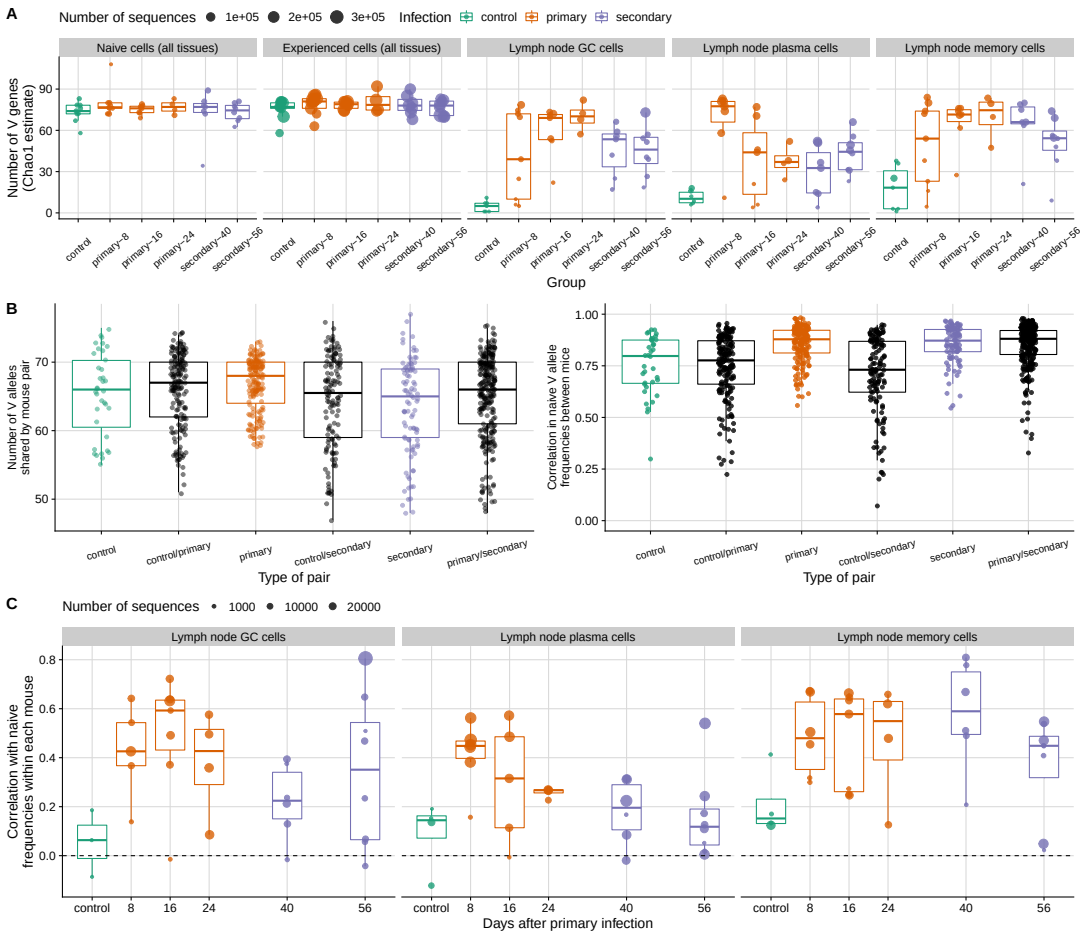

Figure 3. Immunoglobulin V gene usage in the mouse B cell response to influenza infection. (**A**) The number of germline immunoglobulin V alleles is shown for mice infected once or twice with a mouse-adapted H1N1 virus and sacrificed at different time points (8, 16, 24, 40 and 56 days after the primary infection, with the second infection at day 32). Uninfected control mice are shown in red. Each point represents a mouse. At the peak of the response, most alleles present in each mouse are represented in lymph-node germinal center (GC), plasma and memory cells, which were likely induced by the influenza infection. (**B**) Number of V alleles shared by pairs of mice in the naive repertoire (left) and the Pearson correlation in their frequencies for each pair (excluding mice with fewer than 100 reads in the naive repertoire; right). Each point represents a pair. (**C**) Pearson correlation within each mouse between V allele frequencies in influenza-induced populations and frequencies in the naive repertoire. Each point represents a mouse, and solid-line boxplots indicate the distribution in the observed data.

Figure 3–Figure supplement 1. Number of B cells sorted from mice.

Figure 3–Figure supplement 2. Evidence of B cell evolution and competition in infected mice.

Figure 3–Figure supplement 3. High-frequency amino acid mutations in different tissues.

Figure 3–Figure supplement 4. Probability that two B cell lineages sharing the same V allele have high-frequency mutations in common.

Figure 3–Figure supplement 5. Number of high frequency mutations as a function of lineage size in lymph nodes

Figure 3–Figure supplement 6. Similarity of CDR3 sequences sampled from different mice.

Figure 3–Figure supplement 7. Convergent CDR3 sequences from day 56 plasma cells.

Figure 3–Figure supplement 8. Fraction of B cell lineages mostly contained in a single tissue or cell type.

Contingent allele frequencies in the mouse response to influenza infection despite evidence of germline-encoded advantages

We compared these simulated dynamics with the B cell response of C57BL/6 mice infected with influenza virus once or twice and sacrificed at different times points (8, 16, 24, 40 and 56 days after the primary infection, with the secondary infection on day 32; Materials and Methods: "Experimental infection of mice with an influenza A/H1N1 virus"). Because influenza viruses do not naturally infect mice, any germline-encoded specificities for influenza antigens are either evolutionary spandrels or the product of selection to recognize molecular patterns shared between influenza and pathogens that have historically infected mice. We used RNA sequencing to estimate the frequencies of germline alleles and the relative sizes of B cell lineages in each mouse. We focused on heavy-chain sequences sampled from the mediastinal lymph node because, consistent with previous work (***Sealy et al., 2003***), cell sorting data indicated that lymph node B cells were induced by the influenza infection (control mice had very few germinal center, plasma or memory cells in the mediastinal lymph node; ***Figure 3***–***Figure Supplement 1***). Early in the mouse response to influenza, lymph node populations likely consist of extrafollicular plasma cells expanding outside of germinal centers, with germinal-center derived cells arriving later (***Sealy et al., 2003***) and persisting for as long as six months (***Yewdell et al., 2021***). Most germline V alleles observed in a mouse (across all tissues and cell types sampled) were represented in the influenza-induced lymph node populations, suggesting that most mouse V alleles can produce at least some receptors capable of binding influenza antigens (***Figure 3***). To compare the observed mouse responses with our simulations, we measured the correlation in germline V allele frequencies and in their deviations from the naive repertoire between pairs of infected mice (Materials and Methods: "Estimating correlations between mice").

As expected, influenza infection led to competition and affinity maturation in mouse B cell lineages (***Figure 3***–***Figure Supplement 2***). Serum antibody titers against the infecting virus measured by ELISA rose about 1,000 fold between days 8 and 24 and remained high. In parallel to this rise in antibody titers, germinal center and plasma cell populations became increasingly dominated by a few lineages, suggesting that lineages varied in fitness due initial differences in affinity, differences acquired during the lineages' subsequent evolution, or both. Lineages sampled at later time points had more high-frequency amino acid mutations within them (those present in 50% or more of the reads in a lineage). Those mutations include fixed mutations and those potentially rising to fixation via selection for affinity, and they are unlikely to have arisen from sequencing and amplification errors (which we estimate at 1.8 per thousand nucleotide bases; Materials and Methods: "B cell receptor sequencing"). These trends were visible in the lymph nodes of infected mice but not apparent in other tissues or in control mice (***Figure 3***–***Figure Supplement 3***), suggesting they were driven by the influenza infection. (Influenza-specific lineages may have been present in other tissues, but our data do not allow us to distinguish them from lineages elicited by other antigens.)

Plasma cells and germinal center cells were ultimately dominated by lineages using different germline V alleles in different mice, consistent with the role of contingency observed in our simulations. Early in the response, germline allele frequencies in those cell types were correlated between mice (***Figure 4***A, left panel). In both cell types, this initial similarity was likely partly due to the correlated germline frequencies in the naive repertoire (***Figure 3***B). In early plasma cells, it also reflected the consistent overrepresentation of specific germline alleles, suggesting that those alleles contributed to higher affinity or adaptability than did others (***Figure 4***A, ***Figure 4***B). For instance, in day-8 plasma cells, IGHV14-4*01 increased in frequency relative to the naive repertoire in all 6 mice with enough data, becoming the most common V allele in 4 mice and the second most common in the other 2 (***Figure 4***B). In contrast, at later time points for plasma cells (***Figure 4***–***Figure Supplement 1***) and throughout the response for germinal center cells (***Figure 4***–***Figure Supplement 2***), the most common V allele was usually different in different mice, and most germline alleles were overrepresented relative to the naive repertoire in some mice but not in others. These results sug-

gest that while germline-encoded advantages may strongly shape the early B cell response, they do not predict B cell fitness in the long run.

To further test if the effect of germline-encoded advantages was strongest early in the response, we compared the observed patterns with a null model in which a lineage's fitness is independent of which germline V allele it uses, mimicking the equivalent-alleles scenario in our simulations. We did so by keeping the observed distribution of lineage sizes (a proxy for lineage fitness) while randomly assigning each lineage's germline V allele based on naive repertoire frequencies. Early in the plasma cell response, germline alleles were overrepresented much more consistently between mice than expected under this null model, suggesting that the early response was strongly shaped by the advantages associated with using those alleles (***Figure 4–Figure Supplement 3***). Later in the response, however, specific alleles were not overrepresented in different mice more often than expected if lineage fitness was independent of the germline V allele.

In contrast with germinal center and plasma cells, germline allele frequencies in memory cells remained similar between mice (***Figure 4***A) — and similar to naive allele frequencies within each mouse (***Figure 3***C) — throughout the response. Differences between memory cells and the other cell types could be expected if a higher fraction of memory cells is unrelated to the influenza infection (uninfected controls had more memory B cells than plasma or germinal center cells in their lymph nodes, although they had fewer lymph node memory cells than did infected mice; ***Figure 3–Figure Supplement 1***). In addition, these differences between cell types might reflect the relationship between affinity and B cell differentiation. Since activated B cells with low affinity are more likely than others to exit germinal centers and differentiate into memory cells (***Viant et al., 2020***), dominant lineages with high affinity for influenza antigens might contribute less to the memory cell population than they do to the germinal center and plasma cell populations. Consistent with that possibility, the increasing dominance by a few large and mutated lineages seen in germinal center and plasma cells of infected mice was not evident in their memory cells (***Figure 3–Figure Supplement 2***). Without dominance by a few lineages and whatever germline alleles they happen to use, germline allele frequencies in memory B cells might not stray as far from naive repertoire frequencies as do germline allele frequencies in the other cell types. Consistent deviations from the naive repertoire still occur (***Figure 4***A, ***Figure 4–Figure Supplement 4***), as would be expected if using specific germline alleles makes B cell activation more likely. Of the activated B cells using those germline alleles, those cells with lower affinity than the rest might then differentiate into memory B cells soon after activation. For instance, IGHV14-4*01, which was consistently overrepresented relative to the naive repertoire in early plasma cells, was also overrepresented in the memory cells of 50% or more of the mice at every time point (***Figure 4–Figure Supplement 5***).

Germline V alleles consistently overrepresented early in the response have low predicted mutability in CDRs

Our simulations suggest that the consistent overrepresentation of specific germline alleles early in the response is more likely to reflect germline-encoded affinity than germline-encoded adaptability (***Figure 2***). With sequence data alone, we cannot determine if consistently overrepresented germline V alleles do generate receptors with especially high affinity for influenza antigens. We can, however, estimate potential differences in adaptability between germline alleles based on their sequences alone, using estimates of the propensity of different nucleotide motifs to undergo somatic hypermutation (although those estimates were derived from mouse light-chain rather than heavy-chain genes; ***Cui et al. 2016***) (Methods: "Mutability analysis of germline alleles").

We found no clear evidence that germline alleles with higher predicted mutability in the CDRs (which might give those alleles a higher rate of affinity-changing mutations) tended to increase in frequency relative to the naive repertoire (***Figure 4–Figure Supplement 6***). Neither did germline alleles with lower mutability in the structurally-important framework regions (FRs; where mutations are more likely to be deleterious than in CDRs) tend to increase in frequency. Instead, in day-8 plasma cells we found the opposite relationship: germline alleles tended to increase in frequency

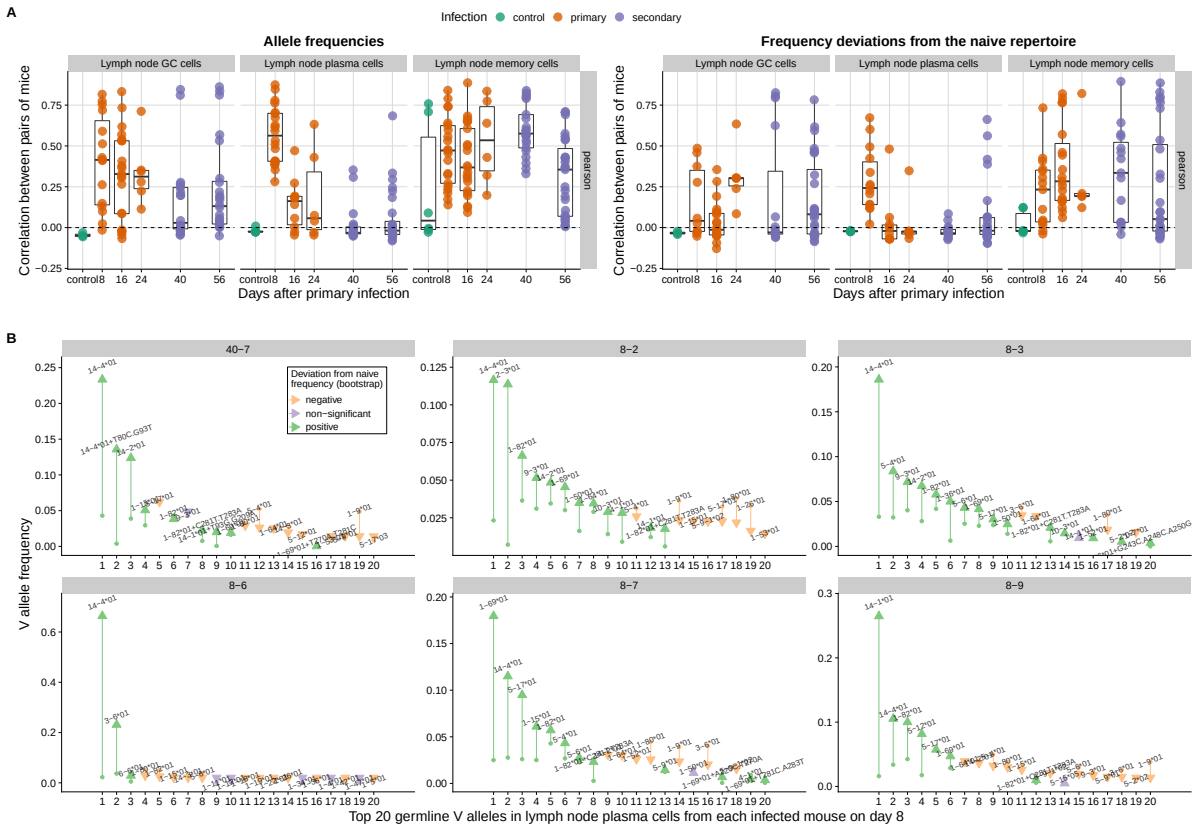

Figure 4. Correlation between mice in the V allele frequencies of influenza-induced populations and in the deviations of those frequencies from the naive repertoire. (**A**) Distribution of pairwise correlations at each time point. Each point represents a pair of mice with at least 100 reads each in the respective B cell population. We computed correlations using Pearson's coefficient and measured frequency deviations as the ratio between a V allele's frequency in an influenza-induced population and its frequency in the naive repertoire. (**B**) Frequency of the 20 most common V alleles in the lymph node plasma cells of each mouse 8 days after primary infection. Each panel represents an individual mouse. The arrows go from each allele's frequency in the naive repertoire to its frequency in lymph node plasma cells. Each allele was labelled as significantly over- or underrepresented in each mouse if the ratio of its experienced and naive frequencies was outside a 95% confidence interval obtained by bootstrap sampling ($n = 500$) of experienced frequencies from the naive repertoire (preserving the observed total number of sequences in each mouse). Mouse 40-7, which was sacrificed 8 days after the secondary infection, was considered a day-8 primary-infection mouse because it showed no signs of infection after the first inoculation and had ELISA titers similar to those of day-8 infected mice.

Figure 4–Figure supplement 1. Top germline V alleles in lymph node plasma cells across time points.

Figure 4–Figure supplement 2. Top germline V alleles in lymph node GC cells across time points.

Figure 4–Figure supplement 3. Between-mouse correlations compared with a null model representing the effects of contingency.

Figure 4–Figure supplement 4. Top germline V alleles in lymph node memory cells across time points.

Figure 4–Figure supplement 5. Alleles consistently overrepresented in early plasma cells shown for other cell types and time points.

Figure 4–Figure supplement 6. Correlation between predicted germline allele mutability and frequency deviations from the naive repertoire

Figure 4–Figure supplement 7. Sensitivity analysis for collapsing identical reads from the same mouse, tissue, cell type and isotype.

Figure 4–Figure supplement 8. Sensitivity analysis using an independent dataset to estimate naive V allele frequencies.

relative to the naive repertoire if they had high mutability in FRs and low mutability in CDRs. The consistently overrepresented and dominant allele IGHV14-4*01, for instance, is predicted to be one of the least mutable in CDRs 1 and 2, (***Figure 4–Figure Supplement 6***). Two other germline alleles consistently overrepresented in day-8 plasma cells, IGHV1-82*01 and IGHV1-69*01 (5 of 6

mice with enough data), have similarly low predicted mutability in CDR1, though not in CDR2. If those alleles do have a high propensity to bind influenza antigens, low mutability in CDRs 1 and 2 might reduce the chance that mutations disrupt this initial binding, potentially reinforcing the fitness advantage of B cells using those alleles.

B cell lineages sharing the same germline V allele rarely had mutations in common

While germinal center cells and plasma cells were increasingly dominated by large lineages with somatic mutations, the sheer number of mutations acquired by a B cell lineage did not predict its success. The biggest lineages in the influenza-induced B cell populations did not generally more mutations than smaller lineages (***Figure 3–Figure Supplement 5***). This observation is consistent with previous work showing that the number of mutations in the B cell receptor does not predict affinity or neutralization strength (***Viant et al., 2020***; ***Sakharkar et al., 2021***; ***Neumeier et al., 2021***). Thus, successful lineages might be those that acquire one or a few substitutions with large effects on affinity, instead of many substitutions with smaller effects.

We found no tendency for these mutations to be the same in B cell lineages using the same germline V allele. Most pairs of lineages with the same V allele had no high-frequency mutations in common (***Figure 3–Figure Supplement 4***). For specific cell types and specific V alleles, we found some instances of high-frequency mutations shared by multiple lineages. However, they were constrained to one or two mice, suggesting they might be an artifact of the incorrect partitioning of a single large lineage into several small ones. Overall, these results suggest that influenza infection does not strongly select the same mutations in B cell lineages with the same germline V alleles. Multiple ways to improve affinity might be possible for the same germline V allele, especially if epistatic interactions between the V segment and the other segments cause the same mutation to have different effects in different lineages.

Limited evidence of selection for specific CDR3 sequences

While binding can occur via the two CDRs solely encoded by the V segment, it often occurs via CDR3, which spans the junction between the segments. Thus, while selection for receptors with specific germline V alleles seems to have a limited effect, influenza antigens might also select for receptors with specific CDR3 sequences. To investigate this possibility, we computed the amino acid sequence and biochemical similarity of CDR3 sequences sampled from different mice and matched for the same length (Methods: "Measuring CDR3 sequence similarity"). On average, length-matched CDR3 sequences from the influenza-induced populations of different mice were no more similar than sequences sampled from their naive repertoires (***Figure 3–Figure Supplement 6***). This result suggests that influenza infection in mice does not strongly select for B cell receptors with particular CDR3 sequences. While individuals exposed to the same pathogen are more likely to share specific CDR3 sequences compared with healthy individuals (***Ortega et al., 2021***), our results suggest those convergent CDR3s do not make up a large fraction of the response.

Finally, influenza antigens might select for combinations of specific germline alleles and CDR3 sequences (***Jackson et al., 2014***; ***Harshbarger et al., 2021***). To investigate this possibility, we computed the similarity of CDR3 sequences from different mice matched both for the same length and the same germline heavy-chain V allele. Length- and allele-matched CDR3 sequences from the lymph node populations of different mice were not, overall, more similar than length- and allele-matched sequences from the naive repertoire (***Figure 3–Figure Supplement 6***). This result suggests that, overall, binding influenza antigens with a specific germline V allele does not require specific CDR3 sequences, even if specific combinations of germline alleles and CDR3 sequences can be found in the response of different individuals (***Jackson et al., 2014***). In day-56 plasma cells, we found higher similarity between length- and allele-matched CDR3 sequences than in the naive repertoire, driven by two clusters of sequences with different lengths (each using a small set of V alleles; ***Figure 3–Figure Supplement 6***, ***Figure 3–Figure Supplement 7***). Collectively, these CDR3 sequences occurred at a very low frequency throughout the response but made up a significant pro-

portion of plasma cell sequences on day 56. Why these combinations of specific CDR3 sequences and specific alleles might have been selected only late into the secondary response is unclear.

Discussion

How much effective B cell responses depend on particular germline immunoglobulin genes versus their subsequent evolution by affinity maturation has important consequences for adaptive immune evolution and vaccination strategies but remains understudied. In simulations, we find that initial germline-encoded advantages are mostly overcome by B cell lineages using different germline alleles in different individuals. These contingent outcomes arise because the growth of B cell lineages also depends on factors that are largely unpredictable, including the timing, order and effect of mutations in different lineages, genetic drift, demographic stochasticity and stochasticity in VDJ recombination. Our simulations and experiments suggest that the effects of contingency increase over time: The longer B cell lineages evolve, the more opportunity there is for differences to accumulate as those processes play out. Like evolution in general (***Gould, 1989***; ***Blount et al., 2018***; ***Xie et al., 2021***; ***Park et al., 2022***), the evolution of B cell repertoires in different individuals experiencing identical primary infections might become decreasingly predictable at the genetic level over time. Yet, as is often the case in other systems (***Lässig et al., 2017***), the resulting phenotype is remarkably predictable: potent antibodies reliably emerge in most individuals, suggesting there are many different ways to achieve high affinity against the same pathogen.

A testable prediction suggested by those results is that germline allele usage might diverge between people following repeated exposures (such as sequential influenza infections or vaccines) or over time during chronic infections (such as HIV). This prediction depends on the extent to which responses to repeated or prolonged infections rely on the reactivation of preexisting memory cells and their reentry into germinal centers (***Li et al., 2012***; ***Andrews et al., 2015***; ***Mesin et al., 2020***; ***Turner et al., 2020***; ***Hoehn et al., 2021***). Divergence in germline allele frequencies might be small if the response to each exposure is dominated by lineages newly recruited from the naive repertoire. In contrast, successive bouts of evolution by recalled B cell lineages might increase the chance that they overcome germline-encoded advantages. Vaccine strategies focused on the recruitment of specific alleles (***McGuire et al., 2014***; ***Jardine et al., 2016***; ***Bonsignori et al., 2017***; ***Lin et al., 2020***) might be hindered in their immediate goal by contingent patterns of allele usage in different people, especially if the strategy involves multiple immunizations or immunizations in people with extensive immune memory.

In addition to varying over time, the similarity of the induced B cell repertoire might also vary with the complexity of the antigen, since antigens encoding multiple epitopes present more potential specificities. Although certain amino acid motifs can make some germline alleles highly polyreactive (***Hwang et al., 2014***; ***Shiroishi et al., 2018***), individual alleles might be unlikely to have a consistent advantage over others across all epitopes in an antigen or all antigens in a pathogen. Thus, germline-encoded specificities might be more apparent in B cells specific for a single epitope than in the set of all B cells binding the antigen or pathogen. Some previous observations are consistent with this hypothesis. For instance, the response to haptens (simple antigens with few potential epitopes) tends to be dominated by one or a few alleles (***Cumano and Rajewsky, 1985***, ***1986***), while the response to complex antigens can use many (***Kuraoka et al., 2016***). Only a handful of germline alleles are represented in monoclonal antibodies specific for narrowly defined sites on influenza hemagglutinin (***Guthmiller et al., 2021***, ***2022***), while tens of alleles are present in monoclonal antibodies that bind different sites on the major domains of the SARS-CoV-2 spike protein (***Robbiani et al., 2020***; ***Sakharkar et al., 2021***). Many germline V alleles are found in monoclonal antibodies against the IsdB protein of *Staphylococcus aureus*, but antibodies targeting each particular epitope tend to use only one or two of them (***Yeung et al., 2016***).

Understanding this variation further requires overcoming limitations of our analyses. Similarity between individuals might decay even faster in genetically diverse outbred populations than in the inbred mice we used in the experiments. In simulations, we varied the strength of contingency by

varying the frequency and the effect size of somatic mutations relative to the variation in affinity from VDJ recombination alone. Although genetic drift, demographic stochasticity and priority effects in the colonization of germinal centers were present in our model, we did not systematically explore their impacts. Understanding the importance of those processes might require longitudinal data to resolve the timing of cell arrivals in germinal centers and the lineages' population dynamics early in the response. Complementing our sequence analysis, affinity measurements could be used to estimate the affinity distributions of naive B cells using different germline alleles, compare variation within and between those distributions, and directly test if alleles with higher-affinity distributions tend to be used by B cell lineages with high growth rates. Affinity measurements could also be used to study germline allele usage in pathogen-specific B cell lineages outside of lymph nodes, which we could not identify with sequence data alone.

Finally, if germline-encoded specificities are most consequential early in the response, long-term selection to "pre-adapt" germline genes might be linked to the benefits of responding rapidly to commonly encountered pathogens. Mathematical models suggest that maintaining innate defenses against a particular pathogen becomes more advantageous the more frequently the pathogen is encountered (***Mayer et al., 2016***). Germline alleles specific to common pathogens or pathogenic motifs might be selected, effectively hardcoding innate defenses into the adaptive immune system (***Collins and Jackson, 2018***). A reliable supply of receptors against common enemies might be especially important in small and short-lived organisms, which can more quickly die of infection and have fewer naive B cells with which to cover the vast space of possible pathogens (***Collins and Jackson, 2018***). Reinforcing germline-encoded specificities might also be especially useful when the opportunity for adaptation is limited, as might be the case for pathogens that induce extrafollicular responses without extensive B cell evolution (although affinity maturation can occur outside of germinal centers; ***Di Niro et al. 2015***; ***Elsner and Shlomchik 2020***). Understanding what conditions favor similar versus contingent allele usage in the antibody repertoire may thus shed light on the long-term evolution of immunoglobulin genes.

Materials and Methods

Model of B cell dynamics

We modeled B cell evolution and competition in germinal centers using stochastic simulations based on a Gillespie algorithm. There are three types of independent events in the model: immigration of individual B cells into germinal centers, cell division and death. The total rate of events λ is given by

$$\lambda = \lambda_{\text{immigration}} + \lambda_{\text{division}} + \lambda_{\text{death}} \quad (1)$$

where the terms on the right-hand side correspond to the rate of each kind of event (mutation is associated with cell division and is therefore not an independent event). The algorithm consists of drawing the time to the next event by sampling from an exponential distribution with rate λ. Once an event has occurred, we a make a second draw to determine its type. The probability for each type of event in this second draw is proportional to the corresponding event-specific rate (e.g., the probability that the next event is a cell division is $\lambda_{\text{division}}/\lambda$). After determining the event type, we update event rates and draw the time to the next event, and so on until a maximum time t_{max} is reached. For each germinal center, we record the number of cells in each B cell lineage (and the V alleles used by the lineages) at the end of day 1 and then every 5 days starting on day 5.

Immigration of B cells into germinal centers is restricted to an initial period with duration t_{imm}. Parameter I_{total} controls the expected number of lineages that enter each germinal center during that time (each recruited B cell is the founder of an individual lineage). Given those parameters, we let $\lambda_{\text{immigration}}$ be a linearly decreasing function over time reaching 0 at t_{imm}, with intercept and slope chosen such that I_{total} lineages are expected to enter each GC by that point ($\lambda_{\text{immigration}}$ then remains at 0 until the end of the simulation).

Once an immigration occurs, we randomly sample a single immigrant from a newly generated recruitment pool of 1,000 naive cells whose V alleles are drawn with replacement from the naive repertoire. For each member of the recruitment pool, we sample an affinity value based on the naive affinity distribution associated with its V allele. By default, all alleles have the same normal affinity distribution with mean and standard deviation equal to 1 (we sample from the associated truncated distribution to avoid negative values). Depending on the scenario, naive B cells using specific V alleles may have a different distribution with mean $1 + s$ and the same standard deviation. The probability that each cell in the recruitment pool is chosen as the new immigrant is then proportional to its affinity.

The rate of cell divisions depends on the total number of cells inside the germinal center, N, and on the rate of cell division for each individual cell, $\mu(N)$:

$$\lambda_{\text{division}}(N) = N \times \mu(N) \tag{2}$$

To represent competition for antigen, $\mu(N)$ decreases with N so that it equals a fixed per-cell death rate δ when the population is at carrying capacity ($N = K$):

$$\mu(N) = \mu_{\text{max}} \times \exp\left[\frac{N}{K}(\ln \delta - \ln \mu_{\text{max}})\right] \tag{3}$$

Once a division event occurs, we randomly sample a B cell to divide. The probability that each is B cell is chosen is proportional to its affinity. Each dividing B cell has some probability of having a mutation that changes affinity by a normally distributed amount with mean 0 and standard deviation β (affinity is set to 0 if the mutation produces a negative value).

Finally, with a fixed per-cell death rate, the population-level death rate is given simply by

$$\lambda_{\text{death}}(N) = N\delta \tag{4}$$

When simulating alleles with higher naive affinity or higher mutation rates than others, we chose the set of 5 alleles present in all mice with average naive frequency of 2-3% (the typical median frequency in the naive repertoire).

Experimental infection of mice with an influenza A/H1N1 virus

We infected 40 8-week-old female C57BL/6 mice weighing 20-22g (8 for each time point) intranasally with 0.5 LD_{50} of a mouse-adapted pandemic H1N1 strain (A/Netherlands/602/2009) in a total of 30 μL of PBS under full anesthesia. In addition, two controls for each time point were given PBS only. All mouse experiments were approved by The University of Chicago Institutional Animal Care and Use Committee (IACUC protocol 71981).

Tissue processing, cell sorting and nucleic acid extraction

We prepared single cell suspensions from the mediastinal lymph node, spleen and both femurs harvested at the indicated time points. B cells were first enriched from the splenocyte suspension by MACS (magnetic activated cell sorting) using the Pan B cell Isolation Kit (Miltenyi Biotec), followed by staining for FACS (fluorescence activated cell sorting). The lymph node and bone marrow cells were directly stained for FACS. Antibodies used for sorting were anti-B220 (clone RA3-6B2, Biolegend), IgD (clone 11-26c.2a, Biolegend), anti-CD4 (clone RM4-5, Biolegend), anti-CD8 (clone 53-6.7, Biolegend), anti-CD38 (clone 90, Biolegend), anti-CD95 (clone Jo-2; BD Biosciences), anti-CD138 (clone 281-2, Biolegend), anti-F4/80 (clone BM8, Biolegend), anti-GL7 (clone GL7, BD Biosciences), anti-Sca-1 (clone D7, Biolegend), and anti-TER-119 (clone TER-119, Biolegend). Antibody stainings were preceded by adding Fc block (anti-CD16/CD32; clone 2.4G2, BD Biosciences). For sorting, the cells were first gated on size and granularity (forward and side scatter, respectively) to exclude debris, followed by doublet exclusion. We sorted naive (IgD+B220+), plasma (IgD-Sca-1hiCD138hi), memory (IgD-B220+CD95-CD38hi) and germinal center (IgD-B220+CD95+ CD38loGL-7+) cells after excluding cells expressing CD4, CD8, TER-199 or F4/80 (to exclude T cells, erythroid cells and

macrophages). After spinning down cells and removing the PBS supernatant, we extracted DNA and RNA from the cell pellets using the AllPrep DNA/RNA Mini Kit (Qiagen), according to the manufacturer's protocol. All samples were kept frozen until sequenced.

B cell receptor sequencing

We generated immunoglobulin heavy chain (IGH) DNA libraries from complementary DNA generated from 10-500 ng of total RNA using Superscript III (Invitrogen) reverse transcriptase and random hexamer primers. For PCR amplifications, we used multiplexed primers targeting the mouse framework region 1 (FR1) of IGHV in combination with isotype-specific primers targeting constant region exon 1 of IgA, IgD, IgE, IgG, or IgM (Table 2). We performed separate PCR reactions for each isotype to avoid formation of inter-isotype chimeric products. We barcoded each sample with 8-mer primer-encoded sequences on both ends of the amplicons and performed PCR amplification in two steps. First, we generated amplicons using primers with the partial Illumina adapter, the sample-specific barcode and the locus-specific sequence. In the second step, we performed another PCR to complete the Illumina adapter sequence and to ensure final products were not amplified to saturation. We purified pooled products by agarose gel electrophoresis and extraction. We used a 600 cycle v3 kit to sequence products using an Illumina MiSeq instrument.

We estimated the rate at which errors were introduced during amplification and sequencing by comparing the sequenced reads with the reference sequence for the corresponding isotype. Because the constant region does not undergo somatic hypermutation, we counted each mismatch between the end of the J gene and the beginning of the conserved region primer as an error introduced by sequencing and amplification. Based on 187,500 errors found out of 104,092,368 bases analyzed, we estimated the error rate to be 1.80 mutations per thousand bases (95% binomial CI 1.79-1.81).

ELISA

We coated 96-well ELISA plates (Thermo Fisher Scientific) overnight at 4°C with eight hemagglutination units (HAU) of virus in carbonate buffer. We used horseradish peroxidase (HRP)-conjugated goat anti-mouse IgG antibody (Southern Biotech) to detect binding of serum antibodies, followed by development with Super Aquablue ELISA substrate (eBiosciences). We measured absorbance at 405 nm on a microplate spectrophotometer (Bio-Rad). We analyzed serum samples starting at a top dilution of 1:20 (PBS controls and day 8 animals) or 1:1000 (all other samples), followed by 2-fold dilutions in 8 (PBS controls and day 8 animals) or 16 steps. We determined the end titer as the last dilution point with an OD value of > 2x the blank average OD value for each respective plate.

Estimating the frequencies of V alleles and B cell lineages

We used *partis* v0.15.0 to partition sequences into lineages and identify the germline alleles used by each lineage's naive ancestor (accounting for variation in the set of germline alleles present in each mouse; ***Ralph and Matsen 2016a***,b, 2019). We used the fraction of reads corresponding to each allele as a proxy for the frequency of that allele in each B cell population. To reduce the error in frequency estimates, we excluded B cell populations with fewer than 100 reads in a mouse. Since we did not barcode individual cells or RNA molecules during sequencing, the number of reads with a particular sequence reflects not only the number of B cells with that sequence but also their transcription levels. However, we found similar results using the number of unique sequences to estimate the abundance of each lineage or allele (i.e., counting multiple identical reads from the same mouse, tissue, cell type and isotype only once; ***Figure 4–Figure Supplement 7***).

We measured the size of each lineage in each lymph-node B cell population as the number of reads from that lineage in that population (as opposed to the number of reads in the lineage across all cell types and tissues). B cell lineages were mostly confined to a single tissue and usually dominated by a single cell type (***Figure 3–Figure Supplement 8***; note that the partitioning of sequences

into lineages was agnostic to cell type and tissue).

While we initially considered Dump-IgD+B220+ cells as naive cells, we noticed that many sequences obtained from them were extensively mutated relative to their inferred germline genes and were also inferred to be part of large clonal expansions. To exclude reads originating from non-naive B cells sorted as IgD+B220+, we considered a read as likely coming from a naive cell if it met all of the following criteria: 1) it came from IgD+B220+ samples; 2) its isotype was IgM or IgD; 3) it belonged to a clone that had a single unique sequence across its reads (and the reads all came from IgD+B220+ samples), and 4) that sequence had at most two nucleotide mutations in the V gene region. To compute naive frequencies, we pooled sequences meeting those criteria across all tissues. When computing experienced-to-naive frequency ratios, we adjusted the frequencies of germline alleles that were sampled in an experienced B cell population but not in naive B cells, since those alleles must have been present in naive B cells even though they were not sampled. In those cases, we imputed a single sequence to the allele in the naive repertoire then recalculated naive allele frequencies accordingly. When computing frequency deviations from the naive repertoire, we excluded mice with fewer than 100 naive reads even if the corresponding experienced population had more than 100 reads.

To test if our results were robust to uncertainty in the identification of naive B cells in our data, we alternatively estimated V allele frequencies from naive B cells (CD138-CD19+IgD++IgM+CD23++ CD21+PI-) sampled by ***Greiff et al.*** (***2017***) from the spleen of healthy C57BL/6 mice. For these data, we processed raw paired-end reads using *presto* v.0.6.2. (***Vander Heiden et al., 2014***), then used *partis* v0.15.0 to identify germline V alleles for a random sample of 20,000 sequences per mouse. V allele frequencies (measured by the fraction of total reads assigned to each gene in each mouse) were positively correlated between this independent dataset and the designated naive populations from our data (mean Spearman correlation coefficient between pairs of mice from each dataset $= 0.68$, interquartile range $0.60 - 0.77$). We repeated the analysis of pairwise frequency-deviation correlations over time after replacing naive frequencies in our mice with the average frequency of each gene in the ***Greiff et al.*** (***2017***) dataset, preserving the number of reads in each mouse. When calculating the average allele frequencies in the alternative data set, we artificially assigned a single read to alleles present in our mice but absent from the alternative data set (since genes present in the experienced cells cannot be entirely missing from the naive repertoire) and re-normalized frequencies so they would sum to 1. Frequency deviations calculated based on this alternative data set were similar to those estimated using our own data (***Figure 4–Figure Supplement 8***).

Estimating correlations between mice

We used Pearson's correlation coefficient to measure the correlation between mice in germline allele frequencies and their deviations from the naive repertoire. Pearson's coefficient was better able to discriminate between different scenarios than Spearman's coefficient, which measures the correlation in frequency deviation ranks instead of using the actual values. In simulations, using Spearman's coefficient leads to a positive correlation in frequency deviations between individuals even in the scenario where all alleles are functionally equivalent (***Figure 2–Figure Supplement 6***). This pattern is driven by the exclusion from the response of alleles with very low naive frequencies (which tend to be the same alleles in different individuals), as those alleles are unlikely to be represented in lineages that successfully establish in germinal centers (repeating the simulations assuming all alleles have identical frequencies in the naive repertoire eliminates this pattern; ***Figure 2–Figure Supplement 6***).

Identifying overrepresented germline alleles

To determine which germline alleles were consistently overrepresented in experienced B cell populations relative to the naive repertoire, we compared the frequency deviations for each germline allele (separately for each type of B cell) with the distribution expected if alleles were sampled based on naive frequencies alone (maintaining the observed the number of sequences in each

mouse). For each germline allele, we then counted the number of mice with stronger deviations from the naive repertoire than expected under this null distribution (using a 95% bootstrap confidence interval).

Mutability analysis of germline alleles

To estimate the mutability of mouse germline V alleles, we used the RS5NF mutability scores estimated by ***Cui et al. 2016*** using non-functional mouse kappa light-chain sequences and implemented in R package *shazam*. These scores describe the relative mutability of all possible 5-nucleotide motifs. We estimated the mutability of each framework region (FR) and complementarity-determining region (CDR) as the average score across motifs in the region. We then calculated an average for all FRs weighted by the length of each FR, and similarly for CDRs. We used *igblast* v1.14.0 to identify the FRs and CDRs of each germline V allele sequence identified by *partis*.

Measuring CDR3 sequence similarity

We compared the amino acid sequence similarity and biochemical similarity of pairs of CDR3 sequences sampled from different mice and matched either for length alone or both for length and V allele. To limit the number of comparisons, we proceeded as follows. For each pair of mice, we chose one mouse and sampled 500 sequences of the same cell type. For each sequence length represented in this sample, we paired sequences from the first sample with randomly chosen sequences of the same length from the second mouse. If matching sequences both for length and V allele, we did this second sampling separately for each combination of V allele and sequence length present in the first sample. This procedure matches sequences while preserving the length distribution (or the joint distribution of length and V alleles) in the first sample.

We measured amino acid sequence similarity as the proportion of sites with the same amino acid in both sequences. Following previous work (***Hershberg and Shlomchik, 2006***; ***Saini and Hershberg, 2015***), we measured biochemical similarity as the proportion of sites in which the amino acids of both sequences belonged to the same category in the classification by (***Chothia et al., 1998***): hydrophobic (F, L, I , M, V, C, W), hydrophilic (Q, R, N, K, D, E) or neutral (S, P, T, A, Y, H, G).

Table 2. Primers for mouse heavy chain B cell receptors.

Primer name	Sequence
P7-VH1-MsFR1-A	CCTGGGGCTTCAGTGA
P7-VH1-MsFR1-B	GCCTGGGACTTCAGTGA
P7-VH1-MsFR1-C	CCTGGGGCCTCAGTGA
P7-VH1-MsFR1-D	GCCTGGGGCTTCAGTAA
P7-VH2-MsFR1	CCCTCACAGAGCCTGT
P7-VH3-MsFR1	CTTCAGGAGTCAGGACCT
P7-VH5-MsFR1-A	GTCCCTGAAACTCTCCTGTG
P7-VH5-MsFR1-B	GCCTGGAAGGTCCGT
P7-VH5-MsFR1-C	GTCCCTGAAACTCTCCTG
P7-VH7-MsFR1	TTCTCTGAGACTCTCCTGTG
P7-VH9-MsFR1	TGGAGAGACAGTCAAGATCTCC
P7-VH10-MsFR1	GATTGGTGCAGCCTAAAGG
P7-VH11-MsFR1	GCTTGGTGCAACCTGG
P7-VH12-MsFR1	TGCTGTCATCAAGCCATCA
P7-VH14-MsFR1	AGTCAAGTTGTCCTGCA
Ms-Tim-IgM	GGGAAGACATTTGGGAAGGAC
Ms-Tim-IgD	TGAGAGGAGGAACATGTCAG
Ms-Inner-IgG1	GCTCAGGGAAATAGCCCTTGAC
Ms-Inner-IgG2	GCTCAGGGAAATAACCCTTGAC
Ms-Inner-IgG2b	ACTCAGGGAAGTAGCCCTTGAC
Ms-Inner-IgG3	GCTCAGGGAAGTAGCCTTTGAC
Ms-Tim-IgA	GTCAGTGGGTAGATGGTGG
Ms-Tim-IgEc	CCAGGCAGCCCAGGGTCATGG

Table 3. PCR conditions.

1st PCR	
usual initial mix	
	per rxn
10x buffer	3 μL
MgCl2	1.8
2mM dNTP	3
v primer	3
c primer	3
template	4μL (200ng total)
Taq	0.3
H20	11.9
total	30

1st PCR cycle	
94°C	7 min
94°C	30s ($\times$ 35 cycles)
56°C	45s
72°C	1.5 min
72°C	10 min

2nd PCR	
MM	10
Q mix	4
f primer	0.4
r primer	0.4
template	0.5
H2O	4.7

2nd PCR cycle	
usual illumina cycling	
95°C	15 min
95°C	30s ($\times$ 12 cycles)
60°C	45s
72°C	1.5 min
72°C	10 min

Data and code availability

Code for the analyses is available at http://github.com/cobeylab/v_gene_selection. Data, intermediate files and results are available on Zenodo (https://doi.org/10.5281/zenodo.7080191). Raw fastq files are available on SRA [Accession number pending].

Competing interests

C.T.S. has consulted for Alvea / Telis Bioscience Inc. on the design of universal influenza vaccines. The other authors report no competing interests.

Acknowledgments

Lauren McGough and Christopher Russo made helpful comments and suggestions to a draft of the manuscript. This project has been funded in part with Federal funds from the National Institute of Allergy and Infectious Diseases, National Institutes of Health, Department of Health and Human Services under grant DP2 AI117921, CEIRS Contract No. HHSN272201400005C and CEIRR contract 75N93021C00015 to S.C., grants R01AI127877, R01AI130398, U19AI057229 to S.D.B and grants U19AI082724, U19AI109946, U19AI057266, CEIRS contract HHSN272201400005C, CEIRR contract 75N93019R00028 and CIVIC contract 75N93019C00051 to P.C.W. The content is solely the responsibility of the authors and does not necessarily represent the official views of the NIAID or the National Institutes of Health. The project was also partly supported by a Complex Systems Scholar Award from the James S. McDonnell Foundation awarded to S.C. M.C.V. was partly supported by a William Rainey Harper Dissertation Fellowship awarded by the University of Chicago. This work was completed in part with resources provided by the University of Chicago Research Computing Center.

References

Andrews SF, Huang Y, Kaur K, Popova LI, Ho IY, Pauli NT, Henry Dunand CJ, Taylor WM, Lim S, Huang M, Qu X, Lee JH, Salgado-Ferrer M, Krammer F, Palese P, Wrammert J, Ahmed R, Wilson PC. Immune history profoundly affects broadly protective B cell responses to influenza. Science translational medicine. 2015 Dec; 7(316):316ra192. http://stm.sciencemag.org/content/7/316/316ra192, doi: 10.1126/scitranslmed.aad0522.

Beatty J, Carrera I. When What Had to Happen Was Not Bound to Happen: History, Chance, Narrative, Evolution. Journal of the Philosophy of History. 2011 Jan; 5(3):471–495. https://brill.com/view/journals/jph/5/3/article-p471_10.xml, doi: 10.1163/187226311X599916, publisher: Brill.

Blount ZD, Lenski RE, Losos JB. Contingency and determinism in evolution: Replaying life's tape. Science. 2018 Nov; https://www.science.org/doi/abs/10.1126/science.aam5979, publisher: American Association for the Advancement of Science.

Bonsignori M, Liao HX, Gao F, Williams WB, Alam SM, Montefiori DC, Haynes BF. Antibody-virus co-evolution in HIV infection: paths for HIV vaccine development. Immunological Reviews. 2017; 275(1):145–160. https://onlinelibrary.wiley.com/doi/abs/10.1111/imr.12509, doi: 10.1111/imr.12509, _eprint: https://onlinelibrary.wiley.com/doi/pdf/10.1111/imr.12509.

Boyer S, Biswas D, Soshee AK, Scaramozzino N, Nizak C, Rivoire O. Hierarchy and extremes in selections from pools of randomized proteins. Proceedings of the National Academy of Sciences. 2016 Mar; 113(13):3482–3487. https://www.pnas.org/content/113/13/3482, doi: 10.1073/pnas.1517813113, publisher: National Academy of Sciences Section: Physical Sciences.

Brack C, Hirama M, Lenhard-Schuller R, Tonegawa S. A complete immunoglobulin gene is created by somatic recombination. Cell. 1978 Sep; 15(1):1–14. http://www.cell.com/article/0092867478900788/fulltext, doi: 10.1016/0092-8674(78)90078-8, publisher: Elsevier.

Chase JM. Community assembly: when should history matter? Oecologia. 2003 Aug; 136(4):489–498. http://link.springer.com/10.1007/s00442-003-1311-7, doi: 10.1007/s00442-003-1311-7.

Chothia C, Gelfand I, Kister A. Structural determinants in the sequences of immunoglobulin variable domain11Edited by A. R. Fersht. Journal of Molecular Biology. 1998 May; 278(2):457–479. https://www.sciencedirect.com/science/article/pii/S0022283698916539, doi: 10.1006/jmbi.1998.1653.

Collins AM, Jackson KJL. On being the right size: antibody repertoire formation in the mouse and human. Immunogenetics. 2018 Mar; 70(3):143–158. https://doi.org/10.1007/s00251-017-1049-8, doi: 10.1007/s00251-017-1049-8.

Collins AM, Yaari G, Shepherd AJ, Lees W, Watson CT. Germline immunoglobulin genes: Disease susceptibility genes hidden in plain sight? Current Opinion in Systems Biology. 2020 Dec; 24:100–108. https://www.sciencedirect.com/science/article/pii/S2452310020300536, doi: 10.1016/j.coisb.2020.10.011.

Crews S, Griffin J, Huang H, Calame K, Hood L. A single VH gene segment encodes the immune response to phosphorylcholine: Somatic mutation is correlated with the class of the antibody. Cell. 1981 Jul; 25(1):59–66. https://www.sciencedirect.com/science/article/pii/0092867481902312, doi: 10.1016/0092-8674(81)90231-2.

Cui A, Niro RD, Heiden JAV, Briggs AW, Adams K, Gilbert T, O'Connor KC, Vigneault F, Shlomchik MJ, Kleinstein SH. A Model of Somatic Hypermutation Targeting in Mice Based on High-Throughput Ig Sequencing Data. The Journal of Immunology. 2016 Nov; 197(9):3566–3574. http://www.jimmunol.org/content/197/9/3566, doi: 10.4049/jimmunol.1502263.

Cumano A, Rajewsky K. Clonal recruitment and somatic mutation in the generation of immunological memory to the hapten NP. The EMBO Journal. 1986 Oct; 5(10):2459–2468. https://onlinelibrary.wiley.com/doi/abs/10.1002/j.1460-2075.1986.tb04522.x, doi: 10.1002/j.1460-2075.1986.tb04522.x.

Cumano A, Rajewsky K. Structure of primary anti-(4-hydroxy-3-nitro-phenyl)acetyl (NP) antibodies in normal and idiotypically suppressed C57BL/6 mice. European Journal of Immunology. 1985; 15(5):512–520. https://onlinelibrary.wiley.com/doi/abs/10.1002/eji.1830150517, doi: 10.1002/eji.1830150517, _eprint: https://onlinelibrary.wiley.com/doi/pdf/10.1002/eji.1830150517.

Das S, Nozawa M, Klein J, Nei M. Evolutionary dynamics of the immunoglobulin heavy chain variable region genes in vertebrates. Immunogenetics. 2008 Jan; 60(1):47–55. https://doi.org/10.1007/s00251-007-0270-2, doi: 10.1007/s00251-007-0270-2.

Desai MM, Fisher DS. Beneficial Mutation–Selection Balance and the Effect of Linkage on Positive Selection. Genetics. 2007 Jul; 176(3):1759–1798. https://doi.org/10.1534/genetics.106.067678, doi: 10.1534/genetics.106.067678.

Di Niro R, Lee SJ, Vander Heiden JA, Elsner RA, Trivedi N, Bannock JM, Gupta NT, Kleinstein SH, Vigneault F, Gilbert TJ, Meffre E, McSorley SJ, Shlomchik MJ. Salmonella Infection Drives Promiscuous B Cell Activation Followed by Extrafollicular Affinity Maturation. Immunity. 2015 Jul; 43(1):120–131. https://www.sciencedirect.com/science/article/pii/S1074761315002575, doi: 10.1016/j.immuni.2015.06.013.

Dunand CJH, Wilson PC. Restricted, canonical, stereotyped and convergent immunoglobulin responses. Philosophical Transactions of the Royal Society B: Biological Sciences. 2015 Sep; 370(1676):20140238. https://royalsocietypublishing.org/doi/full/10.1098/rstb.2014.0238, doi: 10.1098/rstb.2014.0238.

Eisen HN, Siskind GW. Variations in Affinities of Antibodies during the Immune Response. Biochemistry. 1964 Jul; 3(7):996–1008. https://doi.org/10.1021/bi00895a027, doi: 10.1021/bi00895a027, publisher: American Chemical Society.

Elhanati Y, Sethna Z, Marcou Q, Callan CG, Mora T, Walczak AM. Inferring processes underlying B-cell repertoire diversity. Philosophical transactions of the Royal Society of London Series B, Biological sciences. 2015 Sep; 370(1676):20140243. http://rstb.royalsocietypublishing.org/content/370/1676/20140243, doi: 10.1098/rstb.2014.0243.

Elsner RA, Shlomchik MJ. Germinal Center and Extrafollicular B Cell Responses in Vaccination, Immunity, and Autoimmunity. Immunity. 2020 Dec; 53(6):1136–1150. https://www.sciencedirect.com/science/article/pii/S1074761320304933, doi: 10.1016/j.immuni.2020.11.006.

Flajnik MF. Comparative analyses of immunoglobulin genes: surprises and portents. Nature Reviews Immunology. 2002 Sep; 2(9):688. https://www.nature.com/articles/nri889, doi: 10.1038/nri889.

Fukami T. Historical Contingency in Community Assembly: Integrating Niches, Species Pools, and Priority Effects. Annual Review of Ecology, Evolution, and Systematics. 2015; 46(1):1–23. https://doi.org/10.1146/annurev-ecolsys-110411-160340, doi: 10.1146/annurev-ecolsys-110411-160340, _eprint: https://doi.org/10.1146/annurev-ecolsys-110411-160340.

759 **Glanville J**, Kuo TC, von Büdingen HC, Guey L, Berka J, Sundar PD, Huerta G, Mehta GR, Oksenberg JR, Hauser SL,
760 Cox DR, Rajpal A, Pons J. Naive antibody gene-segment frequencies are heritable and unaltered by chronic
761 lymphocyte ablation. Proceedings of the National Academy of Sciences of the United States of America. 2011
762 Dec; 108(50):20066–71. http://www.pnas.org/content/108/50/20066.full, doi: 10.1073/pnas.1107498108.

763 **Gould SJ**. Wonderful Life: The Burgess Shale and the nature of history. New York: Norton; 1989.

764 **Gould SJ**, Lewontin RC. The spandrels of San Marco and the Panglossian paradigm: a critique of
765 the adaptationist programme. Proceedings of the Royal Society of London Series B Biological Sci-
766 ences. 1979 Sep; 205(1161):581–598. https://royalsocietypublishing.org/doi/abs/10.1098/rspb.1979.0086, doi:
767 10.1098/rspb.1979.0086, publisher: Royal Society.

768 **Greiff V**, Menzel U, Miho E, Weber C, Riedel R, Cook S, Valai A, Lopes T, Radbruch A, Winkler TH, Reddy ST. Sys-
769 tems Analysis Reveals High Genetic and Antigen-Driven Predetermination of Antibody Repertoires through-
770 out B Cell Development. Cell Reports. 2017; 19(7):1467–1478. doi: 10.1016/j.celrep.2017.04.054.

771 **Guthmiller JJ**, Han J, Li L, Freyn AW, Liu STH, Stovicek O, Stamper CT, Dugan HL, Tepora ME, Utset HA, Bitar
772 DJ, Hamel NJ, Changrob S, Zheng NY, Huang M, Krammer F, Nachbagauer R, Palese P, Ward AB, Wilson PC.
773 First exposure to the pandemic H1N1 virus induced broadly neutralizing antibodies targeting hemagglutinin
774 head epitopes. Science Translational Medicine. 2021 Jun; 13(596). https://stm.sciencemag.org/content/13/
775 596/eabg4535, doi: 10.1126/scitranslmed.abg4535, publisher: American Association for the Advancement of
776 Science Section: Research Article.

777 **Guthmiller JJ**, Han J, Utset HA, Li L, Lan LYL, Henry C, Stamper CT, McMahon M, O'Dell G, Fernández-Quintero
778 ML, Freyn AW, Amanat F, Stovicek O, Gentles L, Richey ST, de la Peña AT, Rosado V, Dugan HL, Zheng NY,
779 Tepora ME, et al. Broadly neutralizing antibodies target a haemagglutinin anchor epitope. Nature. 2022 Feb;
780 602(7896):314–320. https://www.nature.com/articles/s41586-021-04356-8, doi: 10.1038/s41586-021-04356-8,
781 number: 7896 Publisher: Nature Publishing Group.

782 **Harshbarger WD**, Deming D, Lockbaum GJ, Attatippaholkun N, Kamkaew M, Hou S, Somasundaran M, Wang
783 JP, Finberg RW, Zhu QK, Schiffer CA, Marasco WA. Unique structural solution from a VH3-30 antibody
784 targeting the hemagglutinin stem of influenza A viruses. Nature Communications. 2021 Jan; 12(1):559.
785 https://www.nature.com/articles/s41467-020-20879-6, doi: 10.1038/s41467-020-20879-6, bandiera_abtest: a
786 Cc_license_type: cc_by Cg_type: Nature Research Journals Number: 1 Primary_atype: Research Publisher:
787 Nature Publishing Group Subject_term: Influenza virus;X-ray crystallography Subject_term_id: influenza-
788 virus;x-ray-crystallography.

789 **Hershberg U**, Shlomchik MJ. Differences in potential for amino acid change after mutation reveals distinct
790 strategies for kappa and lambda light-chain variation. Proceedings of the National Academy of Sciences of
791 the United States of America. 2006 Oct; 103(43):15963–8. http://www.ncbi.nlm.nih.gov/pubmed/17038496,
792 doi: 10.1073/pnas.0607581103, publisher: National Academy of Sciences.

793 **Hoehn KB**, Turner JS, Miller FI, Jiang R, Pybus OG, Ellebedy AH, Kleinstein SH. Human B cell lineages engaged
794 by germinal centers following influenza vaccination are measurably evolving. Immunology; 2021.

795 **Hozumi N**, Tonegawa S. Evidence for somatic rearrangement of immunoglobulin genes coding for variable
796 and constant regions. Proceedings of the National Academy of Sciences. 1976 Oct; 73(10):3628–3632. https:
797 //www.pnas.org/content/73/10/3628, doi: 10.1073/pnas.73.10.3628.

798 **Hwang KK**, Trama AM, Kozink DM, Chen X, Wiehe K, Cooper AJ, Xia SM, Wang M, Marshall DJ, Whitesides J, Alam
799 M, Tomaras GD, Allen SL, Rai KR, McKeating J, Catera R, Yan XJ, Chu CC, Kelsoe G, Liao HX, et al. IGHV1-69 B Cell
800 Chronic Lymphocytic Leukemia Antibodies Cross-React with HIV-1 and Hepatitis C Virus Antigens as Well as
801 Intestinal Commensal Bacteria. PLOS ONE. 2014 Mar; 9(3):e90725. https://journals.plos.org/plosone/article?
802 id=10.1371/journal.pone.0090725, doi: 10.1371/journal.pone.0090725, publisher: Public Library of Science.

803 **Jackson KJL**, Kidd MJ, Wang Y, Collins AM. The shape of the lymphocyte receptor repertoire: Lessons from the B
804 cell receptor. Frontiers in Immunology. 2013; 4(SEP):1–12. doi: 10.3389/fimmu.2013.00263, iSBN: 1664-3224
805 (Print)\r1664-3224 (Linking).

806 **Jackson KL**, Liu Y, Roskin K, Glanville J, Hoh R, Seo K, Marshall E, Gurley T, Moody MA, Haynes B, Walter E,
807 Liao HX, Albrecht R, García-Sastre A, Chaparro-Riggers J, Rajpal A, Pons J, Simen B, Hanczaruk B, Dekker C,
808 et al. Human Responses to Influenza Vaccination Show Seroconversion Signatures and Convergent Antibody
809 Rearrangements. Cell Host & Microbe. 2014 Jul; 16(1):105–114. http://www.sciencedirect.com/science/article/
810 pii/S193131281400184X, doi: 10.1016/j.chom.2014.05.013.

Jacob J, Kelsoe G, Rajewsky K, Weiss U. Intraclonal generation of antibody mutants in germinal centres. Nature. 1991 Dec; 354(6352):389–392. https://www.nature.com/articles/354389a0, doi: 10.1038/354389a0, bandiera_abtest: a Cg_type: Nature Research Journals Number: 6352 Primary_atype: Research Publisher: Nature Publishing Group.

Jardine JG, Kulp DW, Havenar-Daughton C, Sarkar A, Briney B, Sok D, Sesterhenn F, Ereño-Orbea J, Kalyuzhniy O, Deresa I, Hu X, Spencer S, Jones M, Georgeson E, Adachi Y, Kubitz M, deCamp AC, Julien JP, Wilson IA, Burton DR, et al. HIV-1 broadly neutralizing antibody precursor B cells revealed by germline-targeting immunogen. Science. 2016 Mar; 351(6280):1458–1463. https://www.science.org/doi/full/10.1126/science.aad9195, doi: 10.1126/science.aad9195, publisher: American Association for the Advancement of Science.

Kuraoka M, Schmidt A, Nojima T, Feng F, Watanabe A, Kitamura D, Harrison S, Kepler T, Kelsoe G. Complex Antigens Drive Permissive Clonal Selection in Germinal Centers. Immunity. 2016 Mar; 44(3):542–552. http://www.cell.com/article/S1074761316300486/fulltext, doi: 10.1016/j.immuni.2016.02.010, publisher: Elsevier.

Li GM, Chiu C, Wrammert J, McCausland M, Andrews SF, Zheng NY, Lee JH, Huang M, Qu X, Edupuganti S, Mulligan M, Das SR, Yewdell JW, Mehta aK, Wilson PC, Ahmed R. Pandemic H1N1 influenza vaccine induces a recall response in humans that favors broadly cross-reactive memory B cells. Proceedings of the National Academy of Sciences. 2012; 109(23):9047–9052. doi: 10.1073/pnas.1118979109, iSBN: 1118979109.

Liao HX, Lynch R, Zhou T, Gao F, Alam SM, Boyd SD, Fire AZ, Roskin KM, Schramm CA, Zhang Z, Zhu J, Shapiro L, Becker J, Benjamin B, Blakesley R, Bouffard G, Brooks S, Coleman H, Dekhtyar M, Gregory M, et al. Co-evolution of a broadly neutralizing HIV-1 antibody and founder virus. Nature. 2013; 496(7446):469–476. http://dx.doi.org/10.1038/nature12053, doi: 10.1038/nature12053, publisher: Nature Publishing Group, a division of Macmillan Publishers Limited. All Rights Reserved.

Lin YR, Parks KR, Weidle C, Naidu AS, Khechaduri A, Riker AO, Takushi B, Chun JH, Borst AJ, Veesler D, Stuart A, Agrawal P, Gray M, Pancera M, Huang PS, Stamatatos L. HIV-1 VRC01 Germline-Targeting Immunogens Select Distinct Epitope-Specific B Cell Receptors. Immunity. 2020 Oct; 53(4):840–851.e6. https://www.cell.com/immunity/abstract/S1074-7613(20)30401-5, doi: 10.1016/j.immuni.2020.09.007, publisher: Elsevier.

Lässig M, Mustonen V, Walczak AM. Predicting evolution. Nature Ecology & Evolution. 2017 Feb; 1(3):1–9. https://www.nature.com/articles/s41559-017-0077, doi: 10.1038/s41559-017-0077, number: 3 Publisher: Nature Publishing Group.

Marchalonis JJ, Schluter SF, Bernstein RM, Shen S, Edmundson AB. Phylogenetic Emergence and Molecular Evolution of the Immunoglobulin Family. In: Dixon FJ, editor. *Advances in Immunology*, vol. 70 Academic Press; 1998.p. 417–506. http://www.sciencedirect.com/science/article/pii/S0065277608603922, doi: 10.1016/S0065-2776(08)60392-2.

Mayer A, Mora T, Rivoire O, Walczak AM. Diversity of immune strategies explained by adaptation to pathogen statistics. Proceedings of the National Academy of Sciences. 2016 Aug; 113(31):8630–8635. https://www.pnas.org/content/113/31/8630, doi: 10.1073/pnas.1600663113.

McCarthy KR, Raymond DD, Do KT, Schmidt AG, Harrison SC. Affinity maturation in a human humoral response to influenza hemagglutinin. Proceedings of the National Academy of Sciences. 2019 Dec; 116(52):26745–26751. https://www.pnas.org/content/116/52/26745, doi: 10.1073/pnas.1915620116, publisher: National Academy of Sciences Section: Biological Sciences.

McGuire AT, Dreyer AM, Carbonetti S, Lippy A, Glenn J, Scheid JF, Mouquet H, Stamatatos L. Antigen modification regulates competition of broad and narrow neutralizing HIV antibodies. Science. 2014 Dec; 346(6215):1380–3. http://www.sciencemag.org/content/346/6215/1380.full, doi: 10.1126/science.1259206.

Mesin L, Schiepers A, Ersching J, Barbulescu A, Cavazzoni CB, Angelini A, Okada T, Kurosaki T, Victora GD. Restricted Clonality and Limited Germinal Center Reentry Characterize Memory B Cell Reactivation by Boosting. Cell. 2020 Jan; 180(1):92–106.e11. http://www.sciencedirect.com/science/article/pii/S0092867419313170, doi: 10.1016/j.cell.2019.11.032.

Neumeier D, Yermanos A, Agrafiotis A, Csepregi L, Chowdhury T, Ehling RA, Kuhn R, Roberto RBD, Tacchio MD, Antonialli R, Starkie D, Lightwood DJ, Oxenius A, Reddy ST. Phenotypic determinism and stochasticity in antibody repertoires of clonally expanded plasma cells. bioRxiv. 2021 Jul; p. 2021.07.16.452687. https://www.biorxiv.org/content/10.1101/2021.07.16.452687v1, doi: 10.1101/2021.07.16.452687, publisher: Cold Spring Harbor Laboratory Section: New Results.

Nielsen SCA, Yang F, Jackson KJL, Hoh RA, Röltgen K, Jean GH, Stevens BA, Lee JY, Rustagi A, Rogers AJ, Powell AE, Hunter M, Najeeb J, Otrelo-Cardoso AR, Yost KE, Daniel B, Nadeau KC, Chang HY, Satpathy AT, Jardetzky TS, et al. Human B Cell Clonal Expansion and Convergent Antibody Responses to SARS-CoV-2. Cell Host and Microbe. 2020; 28(4):516–525.e5. doi: 10.1016/j.chom.2020.09.002.

Ortega MR, Spisak N, Mora T, Walczak AM, Modeling and predicting the overlap of B- and T-cell receptor repertoires in healthy and SARS-CoV-2 infected individuals. bioRxiv; 2021. https://www.biorxiv.org/content/10.1101/2021.12.17.473105v1, doi: 10.1101/2021.12.17.473105, pages: 2021.12.17.473105 Section: New Results.

Pappas L, Foglierini M, Piccoli L, Kallewaard NL, Turrini F, Silacci C, Fernandez-Rodriguez B, Agatic G, Giacchetto-Sasselli I, Pellicciotta G, Sallusto F, Zhu Q, Vicenzi E, Corti D, Lanzavecchia A. Rapid development of broadly influenza neutralizing antibodies through redundant mutations. Nature. 2014 Oct; 516(7531):418–422. http://dx.doi.org/10.1038/nature13764, doi: 10.1038/nature13764, publisher: Nature Publishing Group, a division of Macmillan Publishers Limited. All Rights Reserved.

Park Y, Metzger BPH, Thornton JW. Epistatic drift causes gradual decay of predictability in protein evolution. Science. 2022 May; 376(6595):823–830. https://www.science.org/doi/10.1126/science.abn6895, doi: 10.1126/science.abn6895, publisher: American Association for the Advancement of Science.

Ralph DK, Matsen FA. Consistency of VDJ Rearrangement and Substitution Parameters Enables Accurate B Cell Receptor Sequence Annotation. PLoS computational biology. 2016 Jan; 12(1):e1004409. http://journals.plos.org/ploscompbiol/article?id=10.1371/journal.pcbi.1004409, doi: 10.1371/journal.pcbi.1004409, publisher: Public Library of Science.

Ralph DK, Matsen FA. Likelihood-Based Inference of B Cell Clonal Families. PLOS Computational Biology. 2016 Oct; 12(10):e1005086. https://journals.plos.org/ploscompbiol/article?id=10.1371/journal.pcbi.1005086, doi: 10.1371/journal.pcbi.1005086, publisher: Public Library of Science.

Ralph DK, Matsen FAM. Per-sample immunoglobulin germline inference from B cell receptor deep sequencing data. PLOS Computational Biology. 2019 Jul; 15(7):e1007133. https://journals.plos.org/ploscompbiol/article?id=10.1371/journal.pcbi.1007133, doi: 10.1371/journal.pcbi.1007133.

Robbiani DF, Gaebler C, Muecksch F, Lorenzi JCC, Wang Z, Cho A, Agudelo M, Barnes CO, Gazumyan A, Finkin S, Hägglöf T, Oliveira TY, Viant C, Hurley A, Hoffmann HH, Millard KG, Kost RG, Cipolla M, Gordon K, Bianchini F, et al. Convergent antibody responses to SARS-CoV-2 in convalescent individuals. Nature. 2020 Aug; 584(7821):437–442. https://www.nature.com/articles/s41586-020-2456-9, doi: 10.1038/s41586-020-2456-9, number: 7821 Publisher: Nature Publishing Group.

Rogozin IB, Diaz M. Cutting Edge: DGYW/WRCH Is a Better Predictor of Mutability at G:C Bases in Ig Hypermutation Than the Widely Accepted RGYW/WRCY Motif and Probably Reflects a Two-Step Activation-Induced Cytidine Deaminase-Triggered Process. The Journal of Immunology. 2004 Mar; 172(6):3382–3384. http://www.jimmunol.org/content/172/6/3382.full, doi: 10.4049/jimmunol.172.6.3382, publisher: American Association of Immunologists.

Rogozin IB, Kolchanov NA. Somatic hypermutagenesis in immunoglobulin genes II. Influence of neighbouring base sequences on mutagenesis. Biochimica et Biophysica Acta (BBA) - Gene Structure and Expression. 1992 Nov; 1171(1):11–18. http://www.sciencedirect.com/science/article/pii/016747819290134L, doi: 10.1016/0167-4781(92)90134-L.

Saini J, Hershberg U. B cell Variable genes have evolved their codon usage to focus the targeted patterns of somatic mutation on the complementarity determining regions. Molecular Immunology. 2015 May; 65(1):157–167. http://www.sciencedirect.com/science/article/pii/S0161589015000024, doi: 10.1016/j.molimm.2015.01.001.

Sakharkar M, Rappazzo CG, Wieland-Alter WF, Hsieh CL, Wrapp D, Esterman ES, Kaku CI, Wec AZ, Geoghegan JC, McLellan JS, Connor RI, Wright PF, Walker LM. Prolonged evolution of the human B cell response to SARS-CoV-2 infection. Science Immunology. 2021 Feb; 6(56). https://immunology.sciencemag.org/content/6/56/eabg6916, doi: 10.1126/sciimmunol.abg6916, publisher: Science Immunology Section: Research Article.

Sangesland M, Lingwood D. Public Immunity: Evolutionary Spandrels for Pathway-Amplifying Protective Antibodies. Frontiers in Immunology. 2021; 12. https://www.frontiersin.org/article/10.3389/fimmu.2021.708882.

Sangesland M, Ronsard L, Kazer SW, Bals J, Boyoglu-Barnum S, Yousif AS, Barnes R, Feldman J, Quirindongo-Crespo M, McTamney PM, Rohrer D, Lonberg N, Chackerian B, Graham BS, Kanekiyo M, Shalek AK, Lingwood D. Germline-Encoded Affinity for Cognate Antigen Enables Vaccine Amplification of a Human Broadly Neutralizing Response against Influenza Virus. Immunity. 2019 Oct; 51(4):735–749.e8. https://www.sciencedirect.com/science/article/pii/S1074761319303723, doi: 10.1016/j.immuni.2019.09.001.

Sangesland M, Yousif AS, Ronsard L, Kazer SW, Zhu AL, Gatter GJ, Hayward MR, Barnes RM, Quirindongo-Crespo M, Rohrer D, Lonberg N, Kwon D, Shalek AK, Lingwood D. A Single Human VH-gene Allows for a Broad-Spectrum Antibody Response Targeting Bacterial Lipopolysaccharides in the Blood. Cell Reports. 2020 Aug; 32(8):108065. https://www.sciencedirect.com/science/article/pii/S2211124720310500, doi: 10.1016/j.celrep.2020.108065.

Schulz S, Boyer S, Smerlak M, Cocco S, Monasson R, Nizak C, Rivoire O. Parameters and determinants of responses to selection in antibody libraries. PLOS Computational Biology. 2021 Mar; 17(3):e1008751. https://journals.plos.org/ploscompbiol/article?id=10.1371/journal.pcbi.1008751, doi: 10.1371/journal.pcbi.1008751, publisher: Public Library of Science.

Sealy R, Surman S, Hurwitz JL, Coleclough C. Antibody response to influenza infection of mice: different patterns for glycoprotein and nucleocapsid antigens. Immunology. 2003; 108(4):431–439. https://onlinelibrary.wiley.com/doi/abs/10.1046/j.1365-2567.2003.01615.x, doi: https://doi.org/10.1046/j.1365-2567.2003.01615.x, _eprint: https://onlinelibrary.wiley.com/doi/pdf/10.1046/j.1365-2567.2003.01615.x.

Shiroishi M, Ito Y, Shimokawa K, Lee JM, Kusakabe T, Ueda T. Structure–function analyses of a stereotypic rheumatoid factor unravel the structural basis for germline-encoded antibody autoreactivity. Journal of Biological Chemistry. 2018 May; 293(18):7008–7016. https://www.jbc.org/article/S0021-9258(20)41075-0/abstract, doi: 10.1074/jbc.M117.814475, publisher: Elsevier.

Starr TN, Thornton JW. Epistasis in protein evolution. Protein Science. 2016; 25(7):1204–1218. https://onlinelibrary.wiley.com/doi/abs/10.1002/pro.2897, doi: 10.1002/pro.2897, _eprint: https://onlinelibrary.wiley.com/doi/pdf/10.1002/pro.2897.

Turner JS, Zhou JQ, Han J, Schmitz AJ, Rizk AA, Alsoussi WB, Lei T, Amor M, McIntire KM, Meade P, Strohmeier S, Brent RI, Richey ST, Haile A, Yang YR, Klebert MK, Suessen T, Teefey S, Presti RM, Krammer F, et al. Human germinal centres engage memory and naive B cells after influenza vaccination. Nature. 2020 Oct; 586(7827):127–132. http://www.nature.com/articles/s41586-020-2711-0, doi: 10.1038/s41586-020-2711-0.

Vander Heiden JA, Yaari G, Uduman M, Stern JNH, O'Connor KC, Hafler DA, Vigneault F, Kleinstein SH. pRESTO: a toolkit for processing high-throughput sequencing raw reads of lymphocyte receptor repertoires. Bioinformatics. 2014 Jul; 30(13):1930–1932. https://doi.org/10.1093/bioinformatics/btu138, doi: 10.1093/bioinformatics/btu138.

Viant C, Weymar GHJ, Escolano A, Chen S, Hartweger H, Cipolla M, Gazumyan A, Nussenzweig MC. Antibody Affinity Shapes the Choice between Memory and Germinal Center B Cell Fates. Cell. 2020 Nov; 183(5):1298–1311.e11. https://www.cell.com/cell/abstract/S0092-8674(20)31304-0, doi: 10.1016/j.cell.2020.09.063, publisher: Elsevier.

Victora GD, Nussenzweig MC. Germinal Centers. Annual Review of Immunology. 2012; 30(1):429–457. doi: 10.1146/annurev-immunol-020711-075032, iSBN: 10.1146/annurev-immunol-020711-075032.

Voss WN, Hou YJ, Johnson NV, Delidakis G, Kim JE, Javanmardi K, Horton AP, Bartzoka F, Paresi CJ, Tanno Y, Chou CW, Abbasi SA, Pickens W, George K, Boutz DR, Towers DM, McDaniel JR, Billick D, Goike J, Rowe L, et al. Prevalent, protective, and convergent IgG recognition of SARS-CoV-2 non-RBD spike epitopes. Science. 2021 May; https://science.sciencemag.org/content/early/2021/05/03/science.abg5268, doi: 10.1126/science.abg5268, publisher: American Association for the Advancement of Science Section: Report.

Watson CT, Glanville J, Marasco WA. The Individual and Population Genetics of Antibody Immunity. Trends in Immunology. 2017 Jul; 38(7):459–470. https://www.sciencedirect.com/science/article/pii/S1471490617300625, doi: 10.1016/j.it.2017.04.003.

Wei L, Chahwan R, Wang S, Wang X, Pham PT, Goodman MF, Bergman A, Scharff MD, MacCarthy T. Overlapping hotspots in CDRs are critical sites for V region diversification. Proceedings of the National Academy of Sciences. 2015; p. E728–E737. http://www.pnas.org/lookup/doi/10.1073/pnas.1500788112, doi: 10.1073/pnas.1500788112, iSBN: 1500788112.

West AP, Diskin R, Nussenzweig MC, Bjorkman PJ. Structural basis for germ-line gene usage of a potent class of antibodies targeting the CD4-binding site of HIV-1 gp120. Proceedings of the National Academy of Sciences. 2012 Jul; 109(30):E2083–E2090. https://www.pnas.org/content/109/30/E2083, doi: 10.1073/pnas.1208984109, publisher: National Academy of Sciences Section: PNAS Plus.

Xie VC, Pu J, Metzger BP, Thornton JW, Dickinson BC. Contingency and chance erase necessity in the experimental evolution of ancestral proteins. eLife. 2021 Jun; 10:e67336. https://doi.org/10.7554/eLife.67336, doi: 10.7554/eLife.67336, publisher: eLife Sciences Publications, Ltd.

Yaari G, Vander Heiden JA, Uduman M, Gadala-Maria D, Gupta N, Stern JNH, O'Connor KC, Hafler DA, Laserson U, Vigneault F, Kleinstein SH. Models of somatic hypermutation targeting and substitution based on synonymous mutations from high-throughput immunoglobulin sequencing data. Frontiers in Immunology. 2013 Jan; 4:358. http://journal.frontiersin.org/article/10.3389/fimmu.2013.00358/abstract, doi: 10.3389/fimmu.2013.00358, publisher: Frontiers.

Yeung YA, Foletti D, Deng X, Abdiche Y, Strop P, Glanville J, Pitts S, Lindquist K, Sundar PD, Sirota M, Hasa-Moreno A, Pham A, Melton Witt J, Ni I, Pons J, Shelton D, Rajpal A, Chaparro-Riggers J. Germline-encoded neutralization of a Staphylococcus aureus virulence factor by the human antibody repertoire. Nature Communications. 2016 Nov; 7(1):13376. https://www.nature.com/articles/ncomms13376, doi: 10.1038/ncomms13376, bandiera_abtest: a Cc_license_type: cc_by Cg_type: Nature Research Journals Number: 1 Primary_atype: Research Publisher: Nature Publishing Group Subject_term: Antibodies;Bacterial host response;X-ray crystallography Subject_term_id: antibodies;bacterial-host-response;x-ray-crystallography.

Yewdell WT, Smolkin RM, Belcheva KT, Mendoza A, Michaels AJ, Cols M, Angeletti D, Yewdell JW, Chaudhuri J. Temporal dynamics of persistent germinal centers and memory B cell differentiation following respiratory virus infection. Cell Reports. 2021 Nov; 37(6). https://www.cell.com/cell-reports/abstract/S2211-1247(21)01438-8, doi: 10.1016/j.celrep.2021.109961, publisher: Elsevier.

Yuan M, Liu H, Wu NC, Lee CCD, Zhu X, Zhao F, Huang D, Yu W, Hua Y, Tien H, Rogers TF, Landais E, Sok D, Jardine JG, Burton DR, Wilson IA. Structural basis of a shared antibody response to SARS-CoV-2. Science. 2020 Aug; 369(6507):1119–1123. https://science.sciencemag.org/content/369/6507/1119, doi: 10.1126/science.abd2321, publisher: American Association for the Advancement of Science Section: Report.

Supplementary information

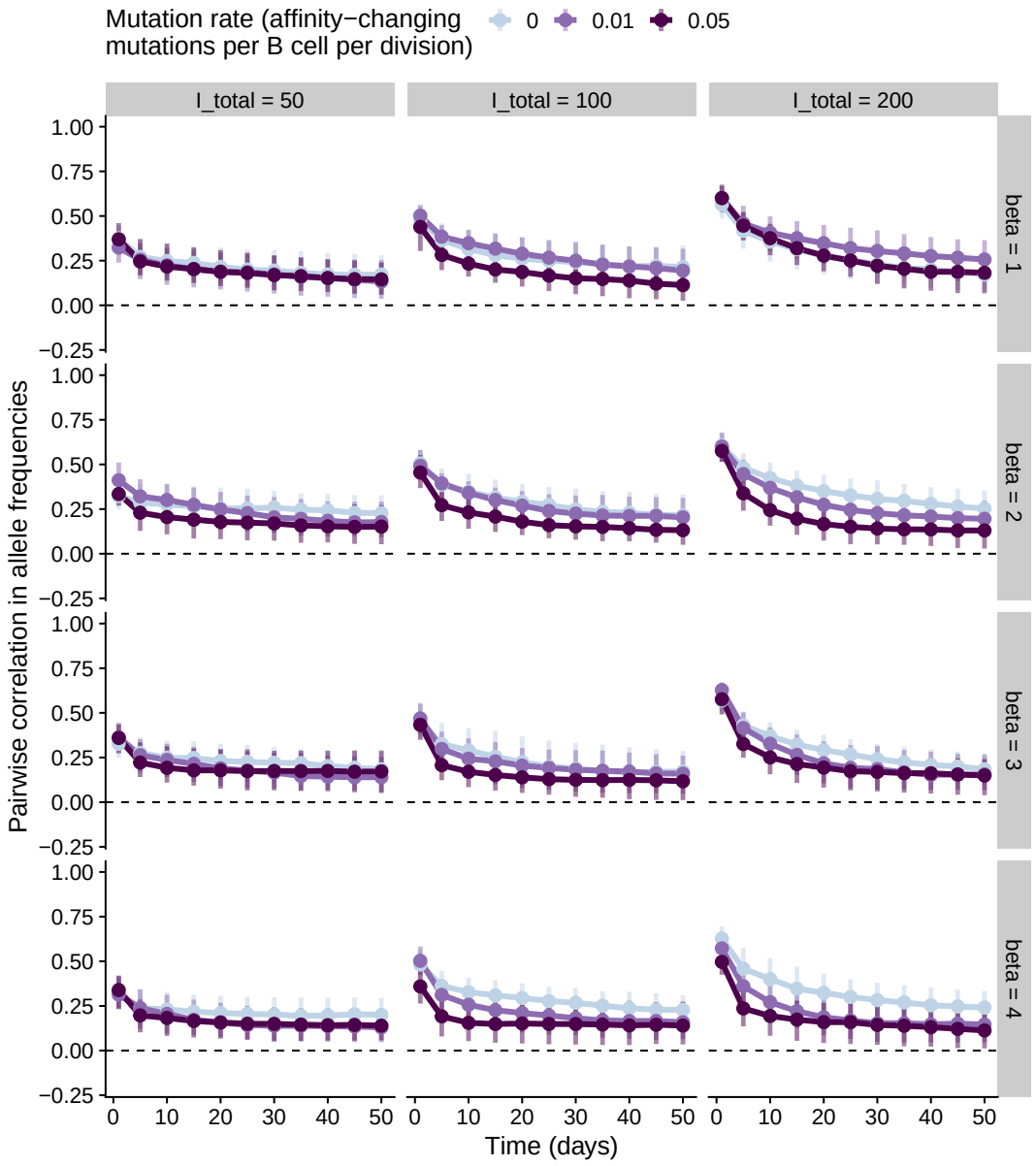

Figure 2–Figure supplement 1. Correlation in allele frequencies between individuals simulated under a scenario where all alleles have identical naive affinity distributions and mutation rates. For each panel, we simulated 20 individuals, each with 15 germinal centers. We varied the rate of affinity-changing mutations per B cell per division (colors), the expected total number of B cell lineages seeding each germinal center (I_{total}, columns) and the standard deviation (β, rows) of the effect size of mutations (which is normally distributed with mean 0). Other parameters were set to the default values in Table 1. Points and vertical bars show the median and the 1st and 4th quartiles computed across all pairs of individuals at each time point.

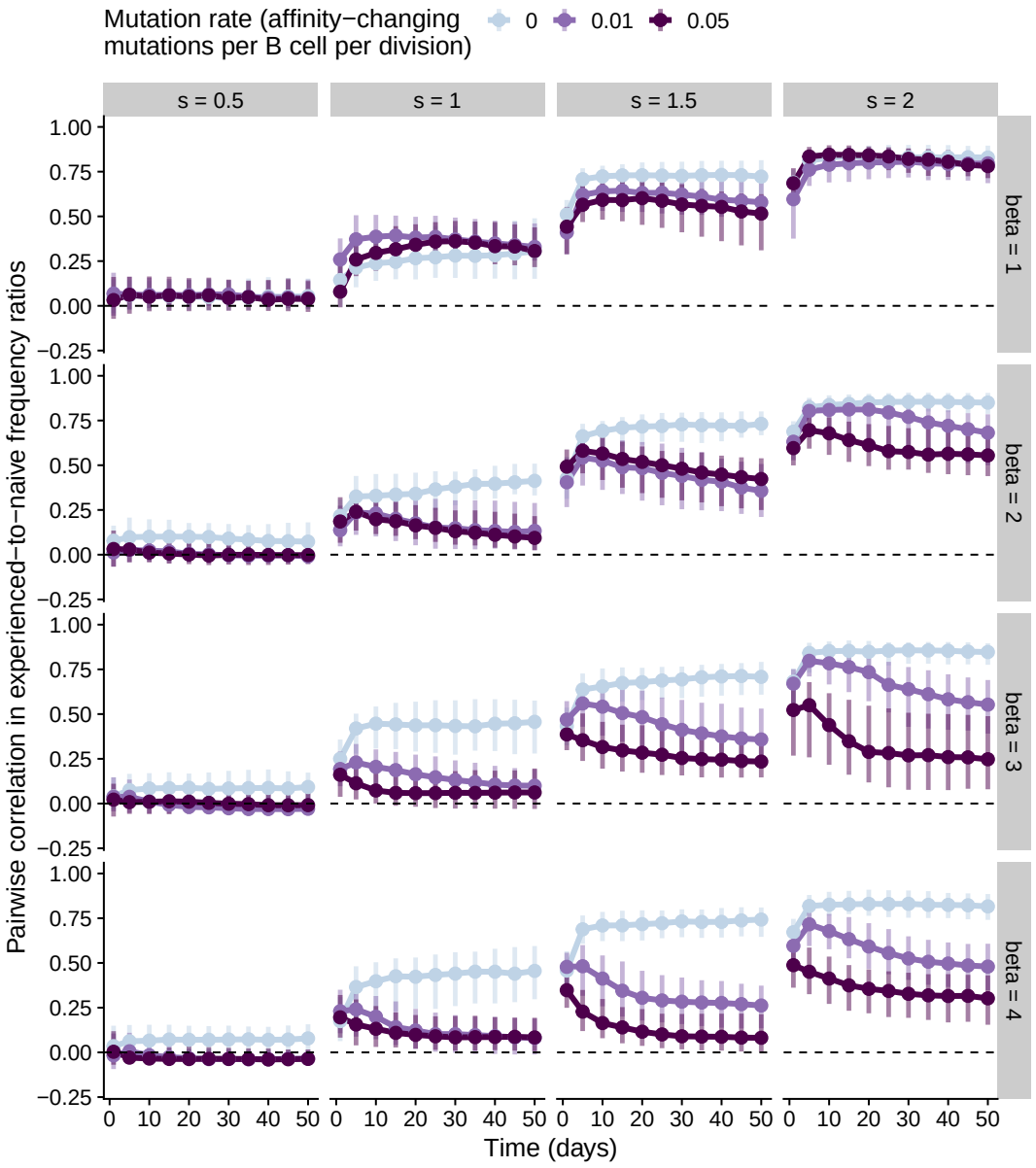

Figure 2–Figure supplement 2. Correlation in allele frequency deviations from the naive repertoire simulated in a scenario where most alleles have identical affinity distributions but five alleles have a different distribution with a higher mean. We measured frequency deviations as the ratio of an allele's frequency across all germinal centers in an individual and its frequency in the individual's naive repertoire. For each panel, we simulated 20 individuals, each with 15 germinal centers. We varied the rate of affinity-changing mutations per B cell per division (colors), the increment in average affinity for high-affinity alleles (s, columns) and the standard deviation (β, rows) of the effect size of mutations (which is normally distributed with mean 0). Other parameters were set to the default values in Table 1. Points and vertical bars show the median and the 1st and 4th quartiles computed across all pairs of individuals at each time point.

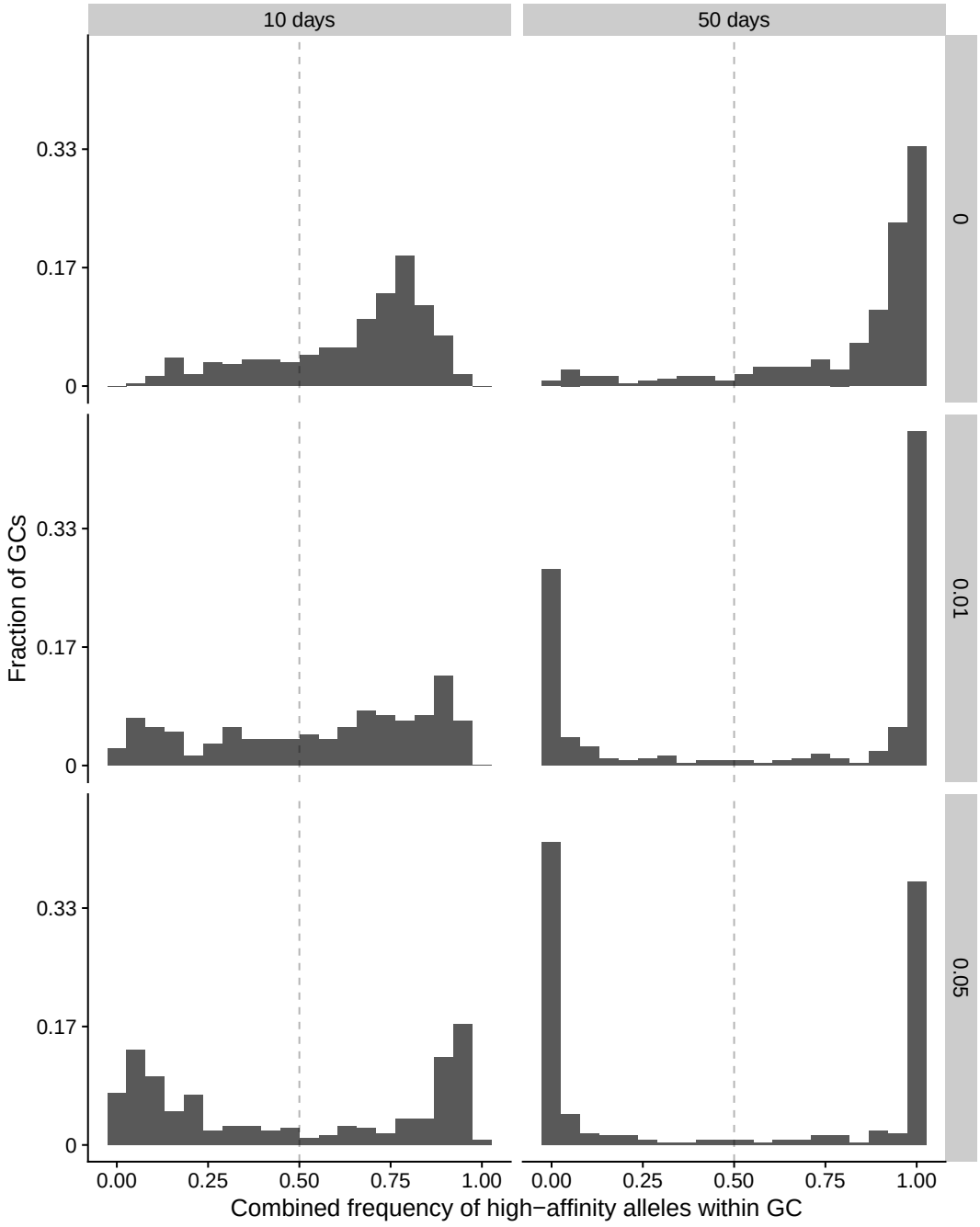

Figure 2–Figure supplement 3. Combined frequency of high-affinity alleles within germinal centers in simulations. Columns show the distribution across germinal centers early (10 days) and late (50 days) in the response. Rows show different somatic hypermutation rates (affinity-changing mutations per B cell per division). For each row, we simulated 20 individuals, each with 15 germinal centers. The same five alleles in all individuals were chosen to have their average naive affinity increased by s = 1.5. Other parameters were set to the default values in Table 1.

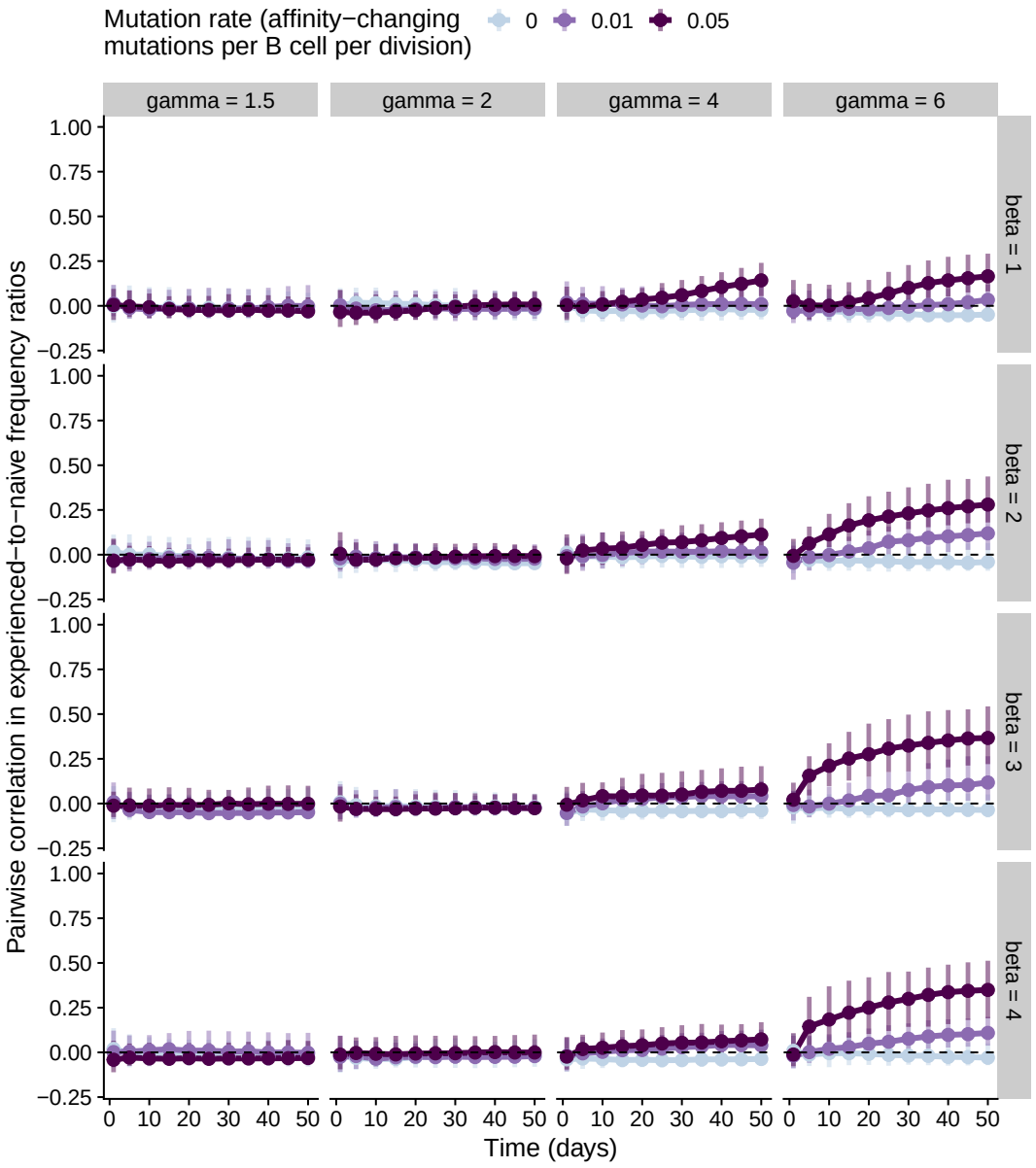

Figure 2–Figure supplement 4. Correlation in allele frequency deviations from the naive repertoire simulated in a scenario where all alleles have have identical affinity distributions but five alleles have a higher mutation rate than the others. We measured frequency deviations as the ratio of an allele's frequency across all germinal centers in an individual and its frequency in the individual's naive repertoire. For each panel, we simulated 20 individuals, each with 15 germinal centers. We varied the rate of affinity-changing mutations per B cell per division (colors), the factor by which the mutation rate increases in high-mutability alleles (γ, columns) and the standard deviation (β, rows) of the effect size of mutations (which is normally distributed with mean 0). Other parameters were set to the default values in Table 1. Points and vertical bars show the median and the 1st and 4th quartiles computed across all pairs of individuals at each time point.

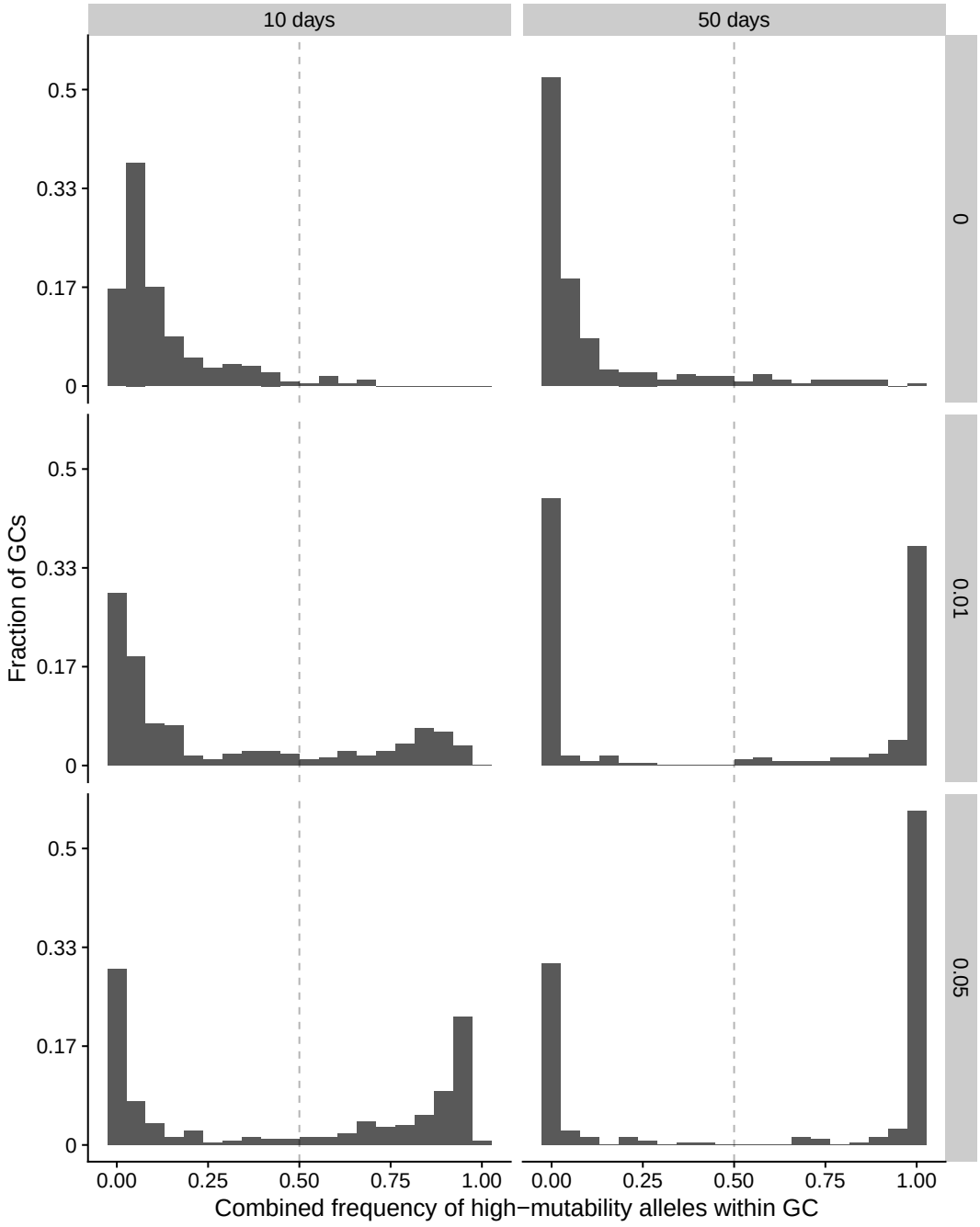

Figure 2–Figure supplement 5. Combined frequency of high-mutability alleles within germinal centers in simulations. Columns show the distribution across germinal centers early (10 days) and late (50 days) in the response. Rows show different somatic hypermutation rates (affinity-changing mutations per B cell per division). For each row, we simulated 20 individuals, each with 15 germinal centers. The same five alleles in all individuals were chosen to have their mutation rate multiplied by a factor γ = 6 relative to other alleles. Other parameters were set to the default values in Table 1.

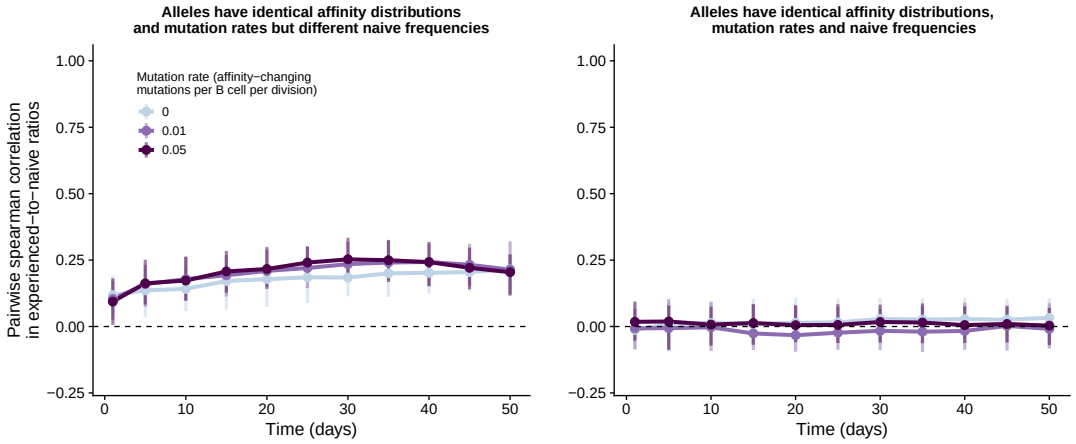

Figure 2–Figure supplement 6. Between-individual correlation in allele frequency deviations from the naive repertoire simulated with (left) and without (right) differences between alleles in their naive repertoire frequencies, measured using the Spearman coefficient. In both cases, all alleles had the same affinity distributions and mutation rates. For each panel, we simulated 20 individuals, each with 15 germinal centers. We varied the rate of affinity-changing mutations per B cell per division (colors). Other parameters were set to the default values in Table 1. Points and vertical bars represent the median and the 1st and 4th quartiles, respectively.

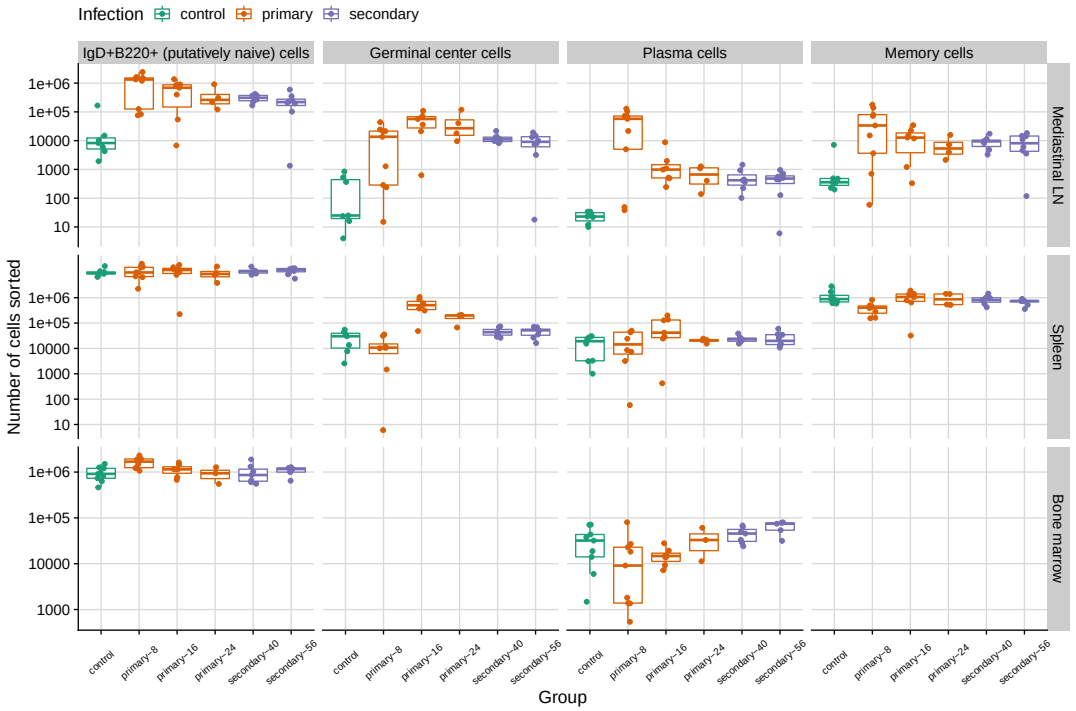

Figure 3–Figure supplement 1. Number of cells sorted from different tissues in mice infected with influenza and in uninfected controls. Infected mice were subject to one or two infections and sacrificed at 8, 16, 24, 40 or 56 days after primary infection. Mice from the last two time points were given a second infection 32 days after the first one.

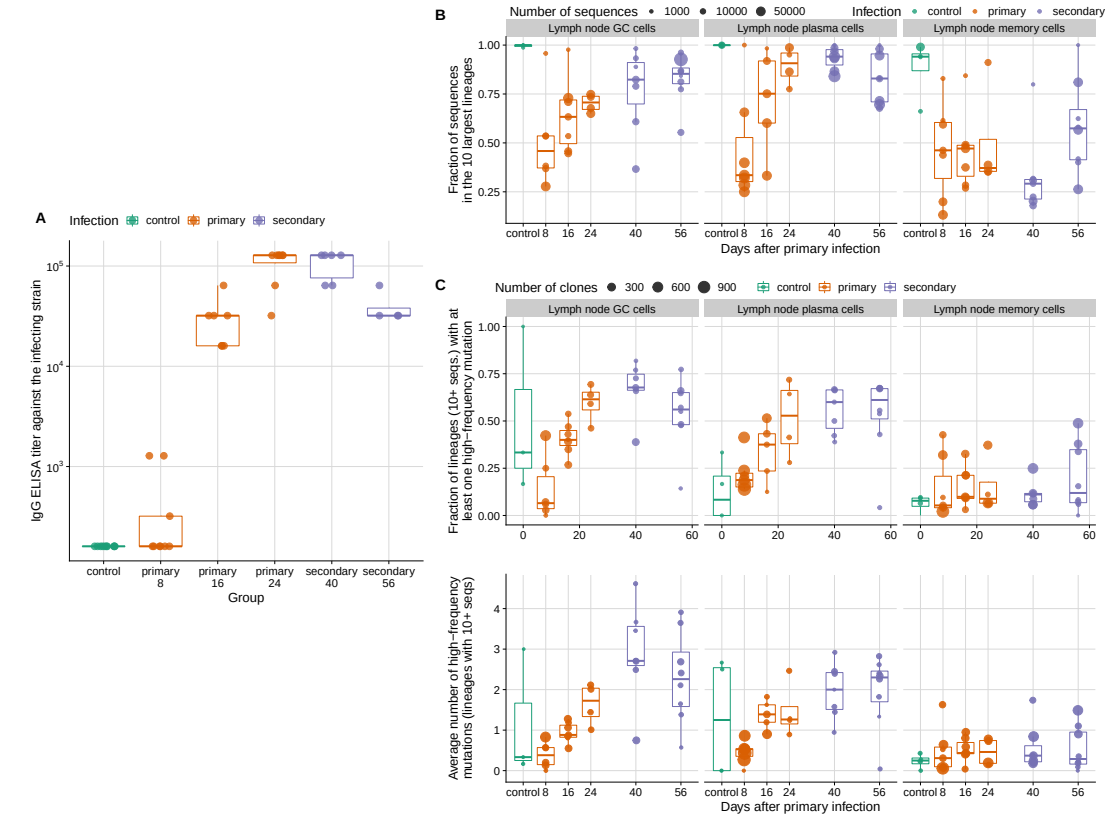

997

Figure 3–Figure supplement 2. Evidence of increased B cell evolution and competition over time in the infected mice. (**A**) Serum antibody titers against the infecting strain measured by ELISA. (**B**) Total fraction of reads in influenza-induced populations represented by the ten largest B lineages in each mouse. The ten largest lineages were chosen based on the number of reads each lineage had in the respective cell type in the lymph node (not the total number of reads each lineage had across all tissue and cell types). (**C**) Fraction of lineages with at least one amino acid mutation at frequency 50% of higher in the lineage (top panel), and the average number of such high-frequency mutations per lineage within each mouse (bottom panel). Mutation frequencies in each lineage were calculated relative to the lineage's number of reads in the respective tissue and cell type combinations. For these calculations, only lineages with at least 10 reads were considered.

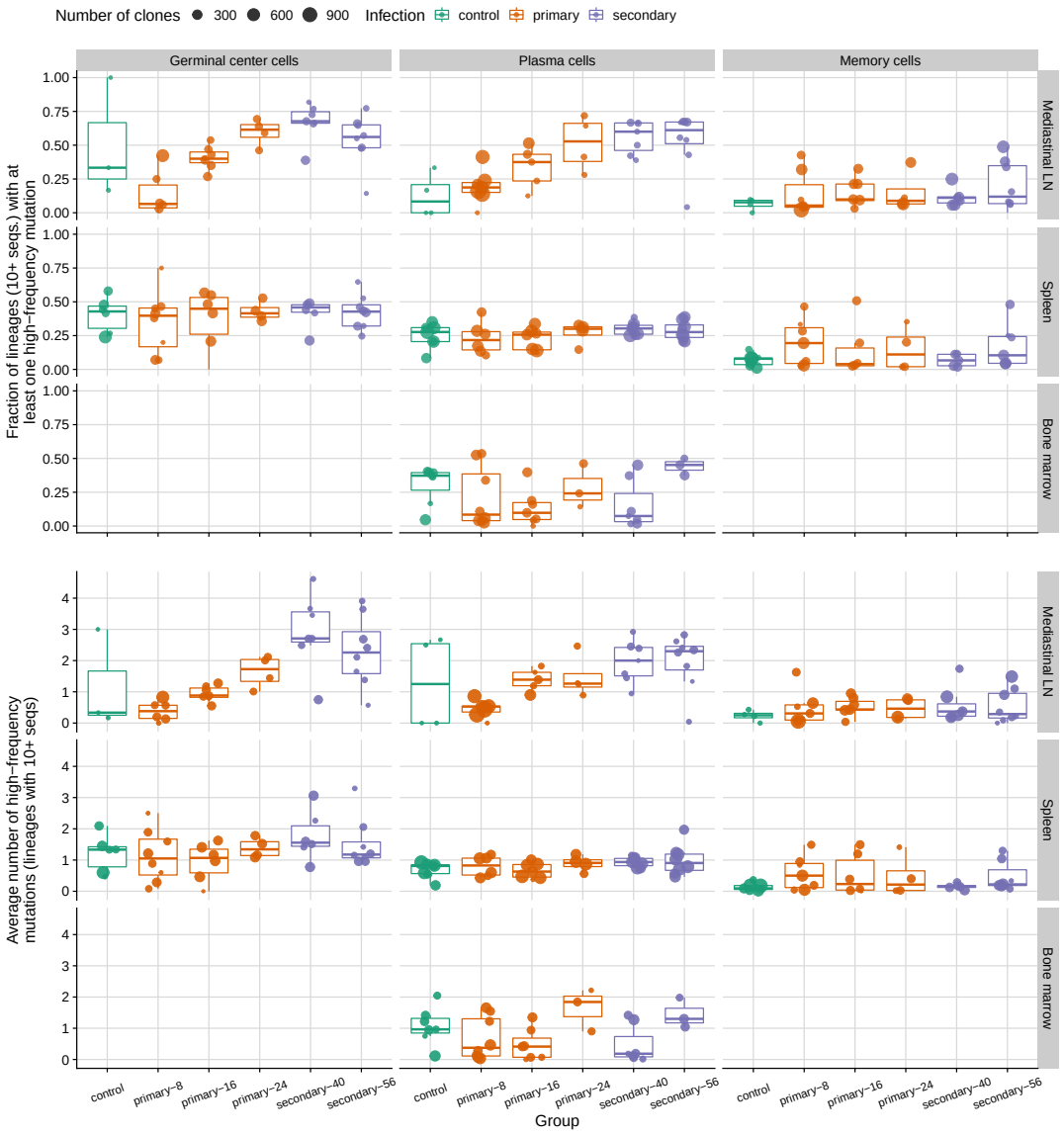

998

Figure 3–Figure supplement 3. Increasing dominance by mutated clones over time is evident in lymph nodes but not in other tissues. Fraction of clones with at least one amino acid mutation at frequency 50% of higher (top panel) and the average number of such high-frequency mutations per clone (bottom panel) for different cell types and tissues. Mutation frequencies in each clone were calculated relative to the clone's number of reads in the respective tissue and cell type combinations (not the total number of reads in the clone across all subtypes and tissues). For each combination of cell type and tissue, each point corresponds to a mouse. Only clones with at least ten reads were considered.

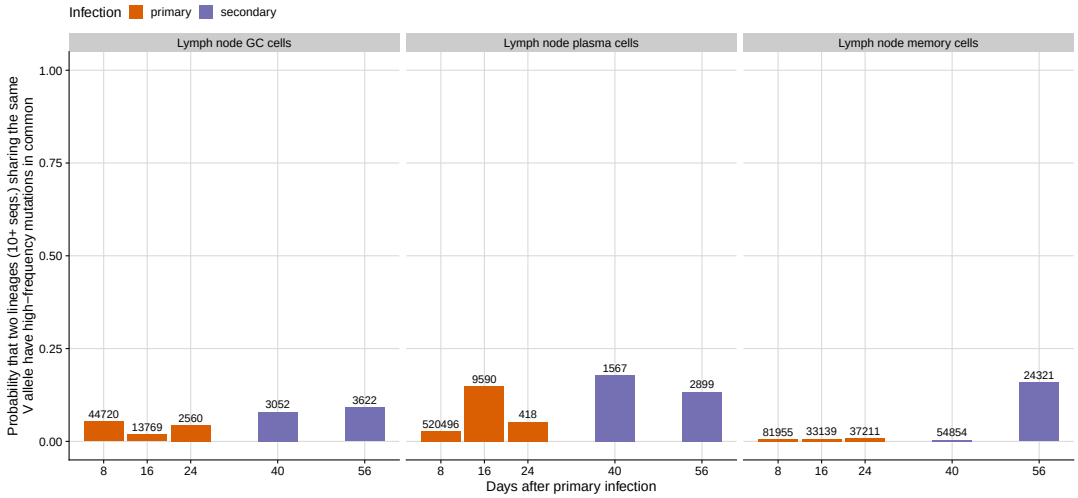

Figure 3–Figure supplement 4. Probability that two B cell lineages sharing the same heavy chain V allele have high-frequency mutations in common. Panels represent B cell types from the lymph node of mice infected with influenza virus (GC: germinal center cells, PC: plasma cells, mem: memory cells). High-frequency mutations were those with a frequency of 50% within the lineage (considering lineage reads in each cell type). The numbers above the bars indicate the number of lineage pairs being compared (pairs were from either the same mouse or difference mice). We restricted the analysis to lineages with at least 10 reads.

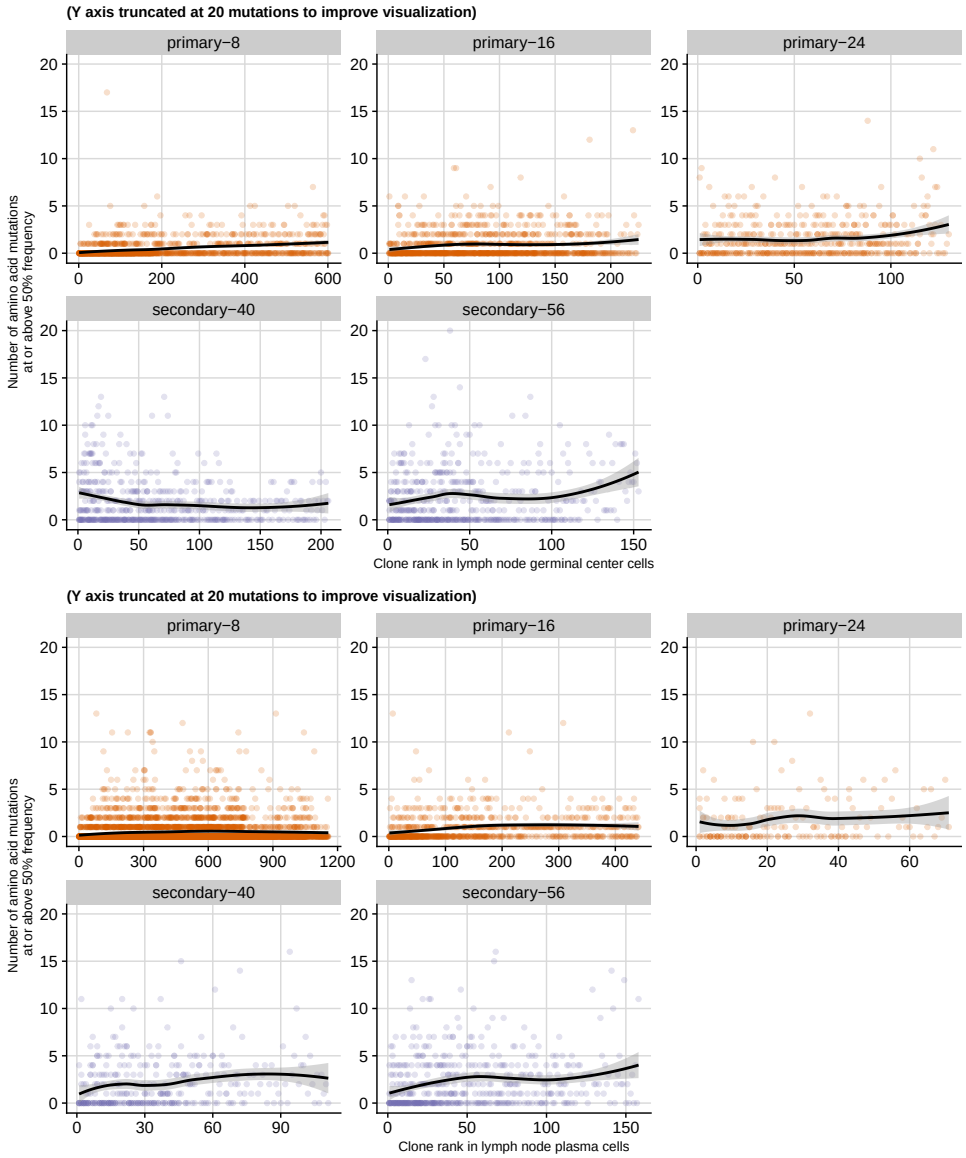

Figure 3–Figure supplement 5. Number of high frequency mutations as a function of clone rank in lymph node germinal center cells (top) and lymph node plasma cells (bottom). Each point represents a clone. Mice from each time point (8, 16, 24, 40 and 56 days after primary infection with influenza) were pooled together in each panel. Clone rank was determined based on the number of reads each clone had in the respective population (lymph node germinal center cells or lymph node plasma cells), not the total number of reads in the clone across all cell types and tissues (the largest clone was assigned rank 1). The solid line is a locally estimated scatterplot smoothing (LOESS) spline.

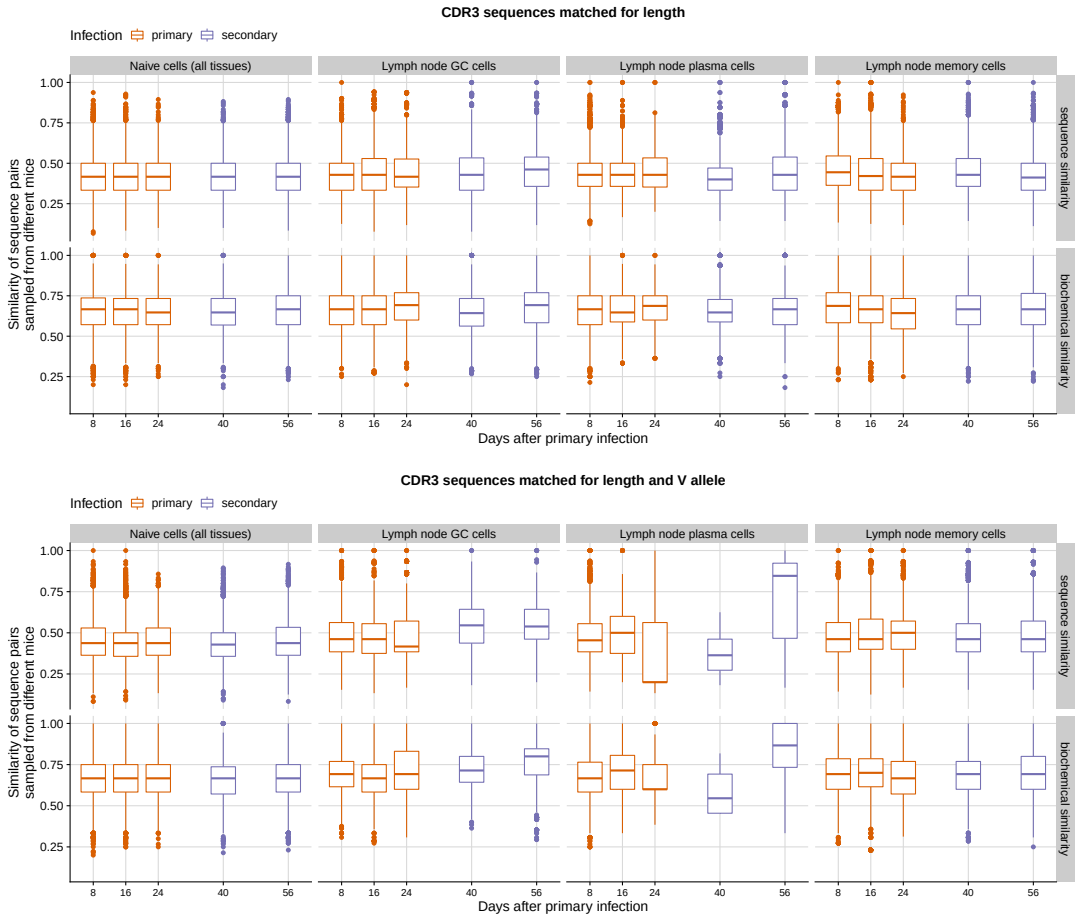

1001

Figure 3–Figure supplement 6. Similarity of CDR3 sequence pairs sampled from different mice and matched for the same length (top) or the same length and the same V allele (bottom). Boxplots show the distribution across sequence pairs from all mouse pairs for each time point (separately for different cell types). Values that fall outside 1.5 times the inter-quartile range are shown as individual points.

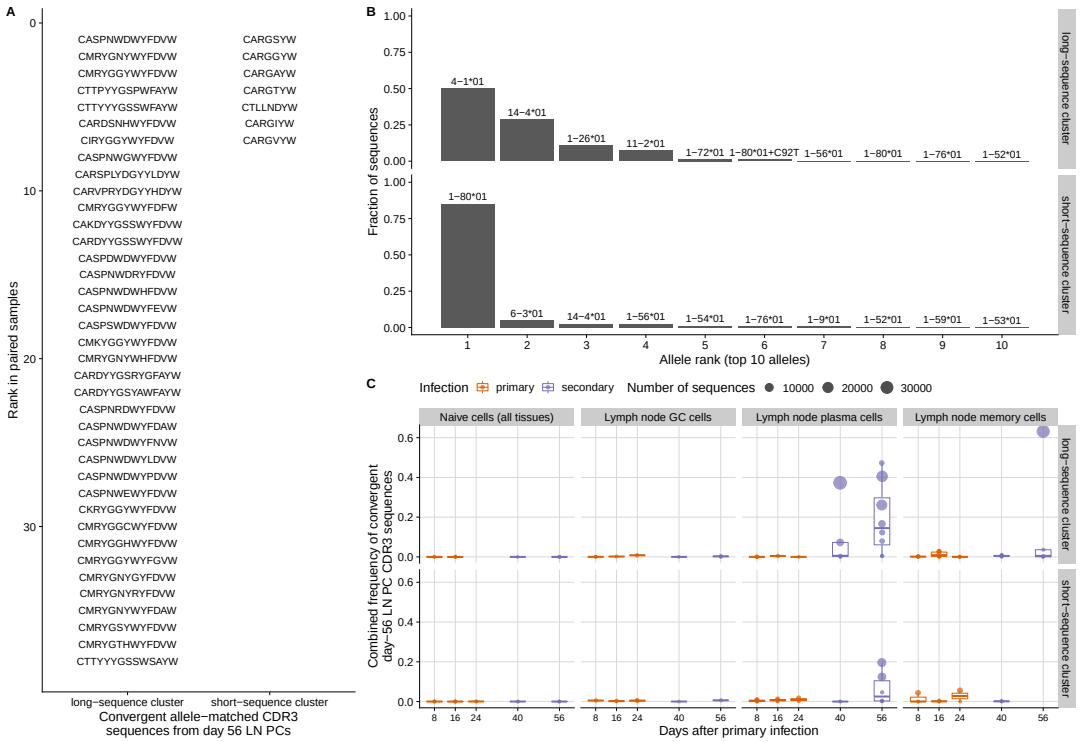

Figure 3–Figure supplement 7. (**A**) Convergent allele-matched CDR3 sequences from day 56 plasma cells of different mice. We included CDR3 sequences from pairs with 75% amino sequence similarity or higher. (**B**) the distribution of the heavy-chain V alleles used by those sequences in day 56 plasma cells (pooled across mice). (**C**) the combined frequency of the sequences in infected mice for all time points. Each points corresponds to an individual mouse.

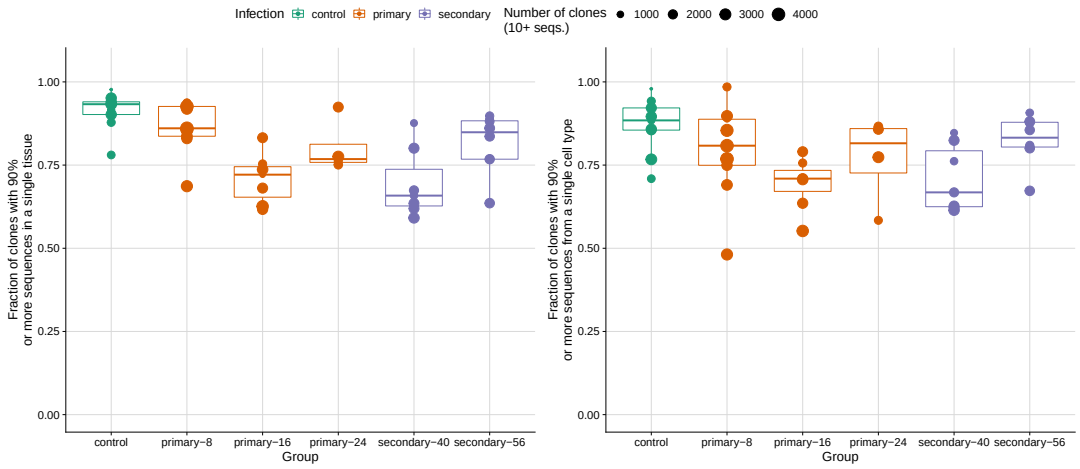

Figure 3–Figure supplement 8. Fraction of clones (with at least 10 reads) that have 90% or more reads from a single tissue (left) or 90% or more reads from a single cell type (right). Each point represents a mouse.

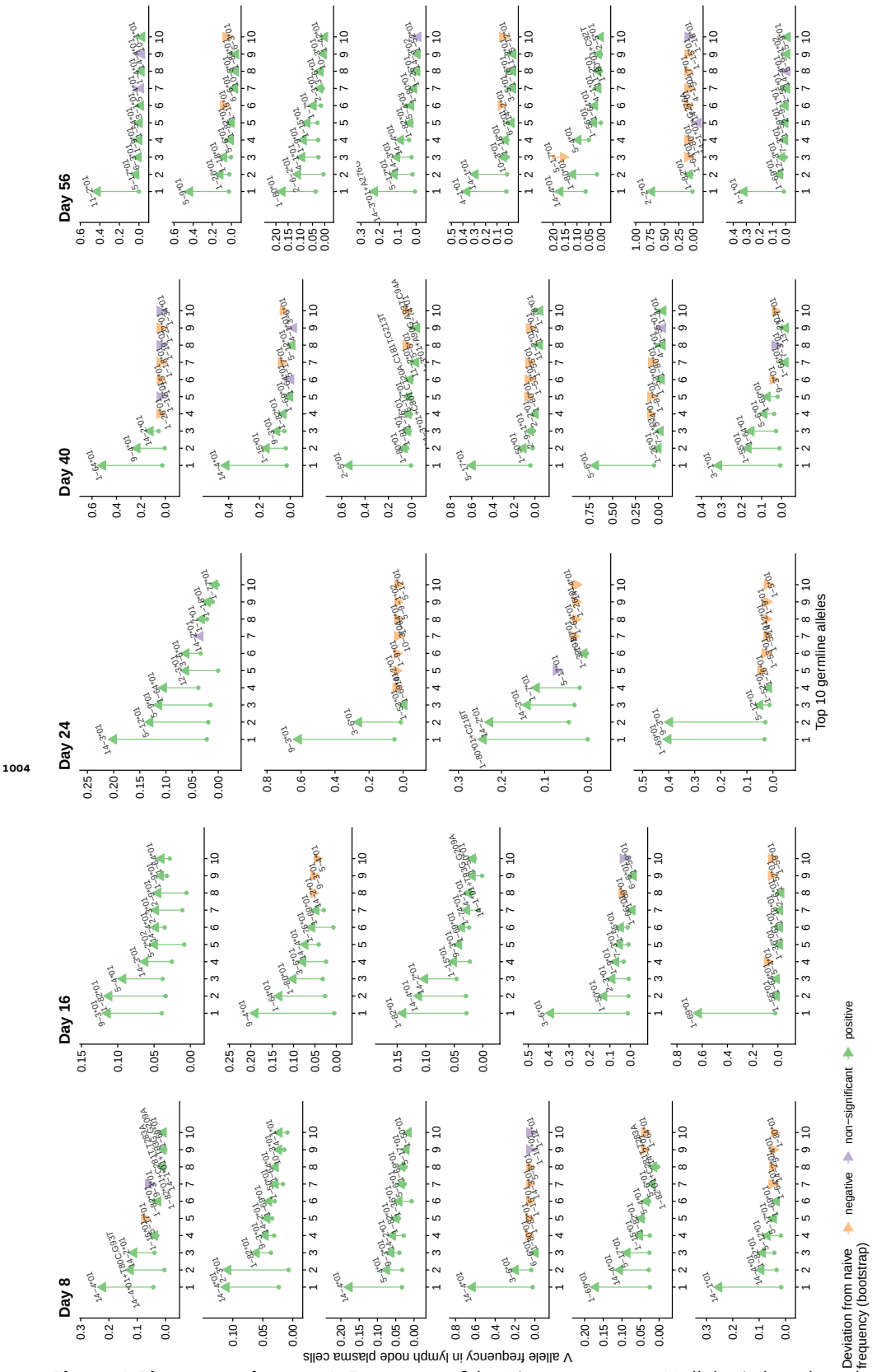

Figure 4–Figure supplement 1. Frequency of the 10 most common V alleles in lymph node plasma cells of infected mice. Each panel represents an individual mouse. The arrows go from each allele's frequency in the naive repertoire to its frequency in lymph node plasma cells. Mouse 40-7, which was sacrificed 8 days after the secondary infection, was considered a day-8 primary-infection mouse because it showed no signs of infection after the first inoculation and had ELISA titers similar to those of day-8 infected mice.

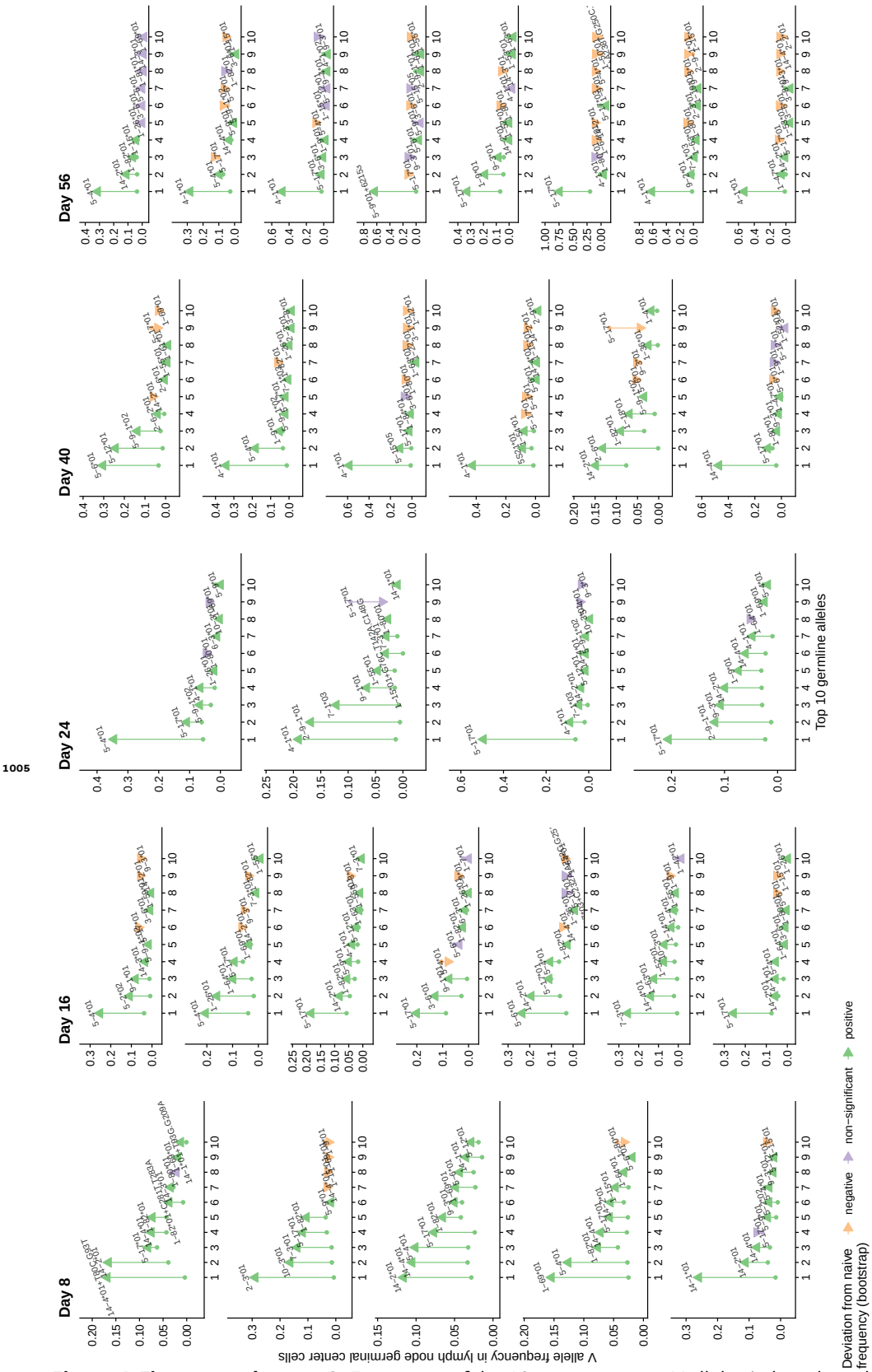

Figure 4–Figure supplement 2. Frequency of the 10 most common V alleles in lymph node germinal center cells of infected mice. Each panel represents an individual mouse. The arrows go from each allele's frequency in the naive repertoire to its frequency in lymph node plasma cells. Mouse 40-7, which was sacrificed 8 days after the secondary infection, was considered a day-8 primary-infection mouse because it showed no signs of infection after the first inoculation and had ELISA titers similar to those of day-8 infected mice.

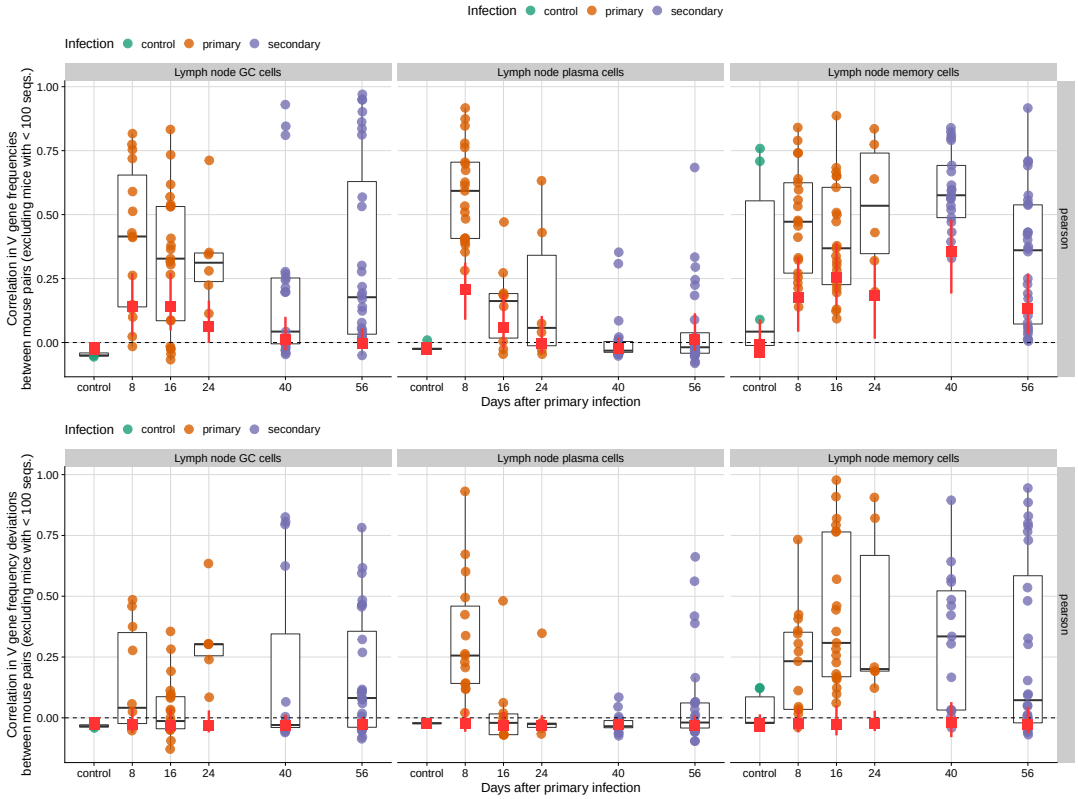

Figure 4–Figure supplement 3. Between-mouse correlations compared with a null model representing the effects of contingency. Each orange or purple point represents the observed correlation between single pair of mice, with boxplots summarizing the observed distributions. Red points and lines represent the median and the first and third quartiles of the distribution generated under the null model ($n = 500$), which maintains the observed distribution of lineage sizes but randomly assigns each lineage a germline V allele based on allele frequencies in the naive repertoire. Null distributions were pooled across replicate realizations and mouse pairs. We computed correlations using Pearson's coefficient and measured frequency deviations as the ratio between a V allele's frequency in an influenza-induced population and its frequency in the naive repertoire.

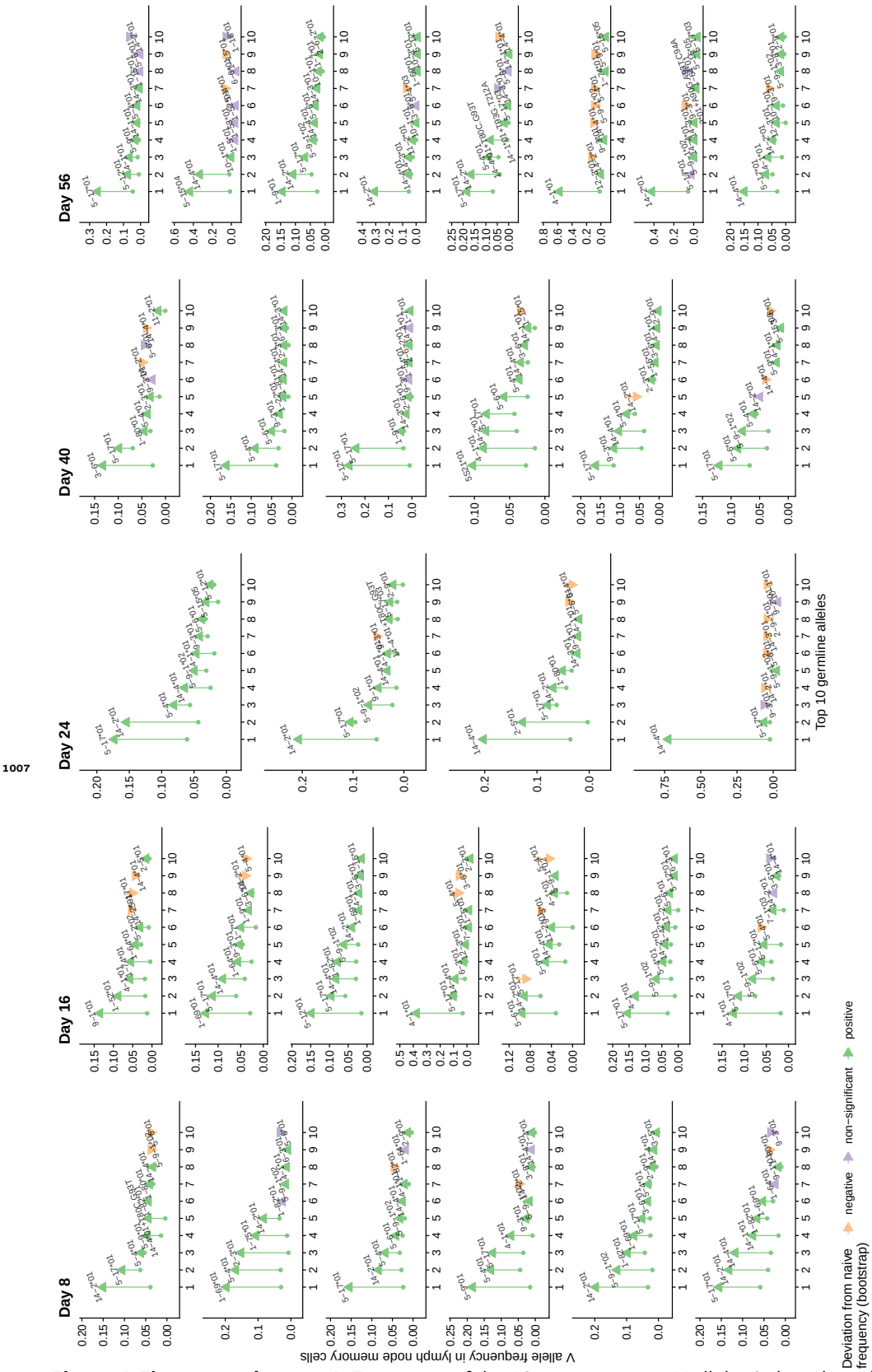

Figure 4–Figure supplement 4. Frequency of the 10 most common V alleles in lymph node memory cells cells of infected mice. Each panel represents an individual mouse. The arrows go from each allele's frequency in the naive repertoire to its frequency in lymph node plasma cells. Mouse 40-7, which was sacrificed 8 days after the secondary infection, was considered a day-8 primary-infection mouse because it showed no signs of infection after the first inoculation and had ELISA titers similar to those of day-8 infected mice.

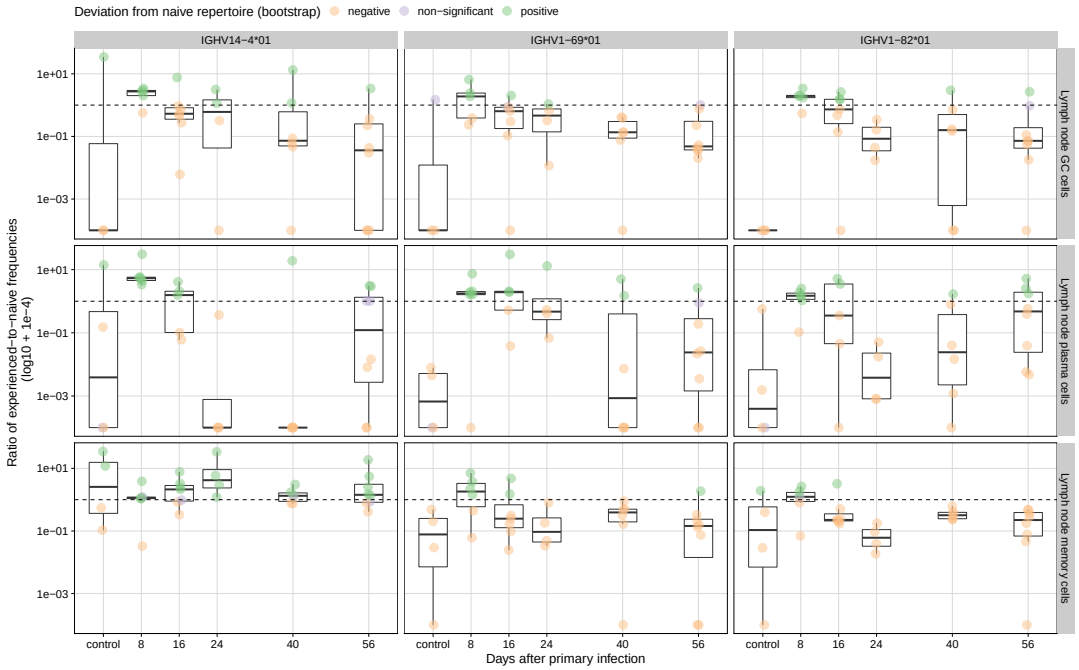

Figure 4–Figure supplement 5. Frequency deviations from the naive repertoire for germline heavy-chain V alleles IGHV14-4*01, IGHV1-82*01 and IGHV1-69*01 at different time points and in different cell types. We measured frequency deviations as the ratio of the experienced-to-naive frequencies in each population. Each point represents a mouse with at least 100 sequences sampled from the corresponding experienced population and from the naive repertoire. Deviations from the naive repertoire are colored based on whether they are different from a null distribution obtained by bootstrapping experienced frequencies from the naive repertoire ($n = 500$ replicates) based on a 95% confidence interval test.

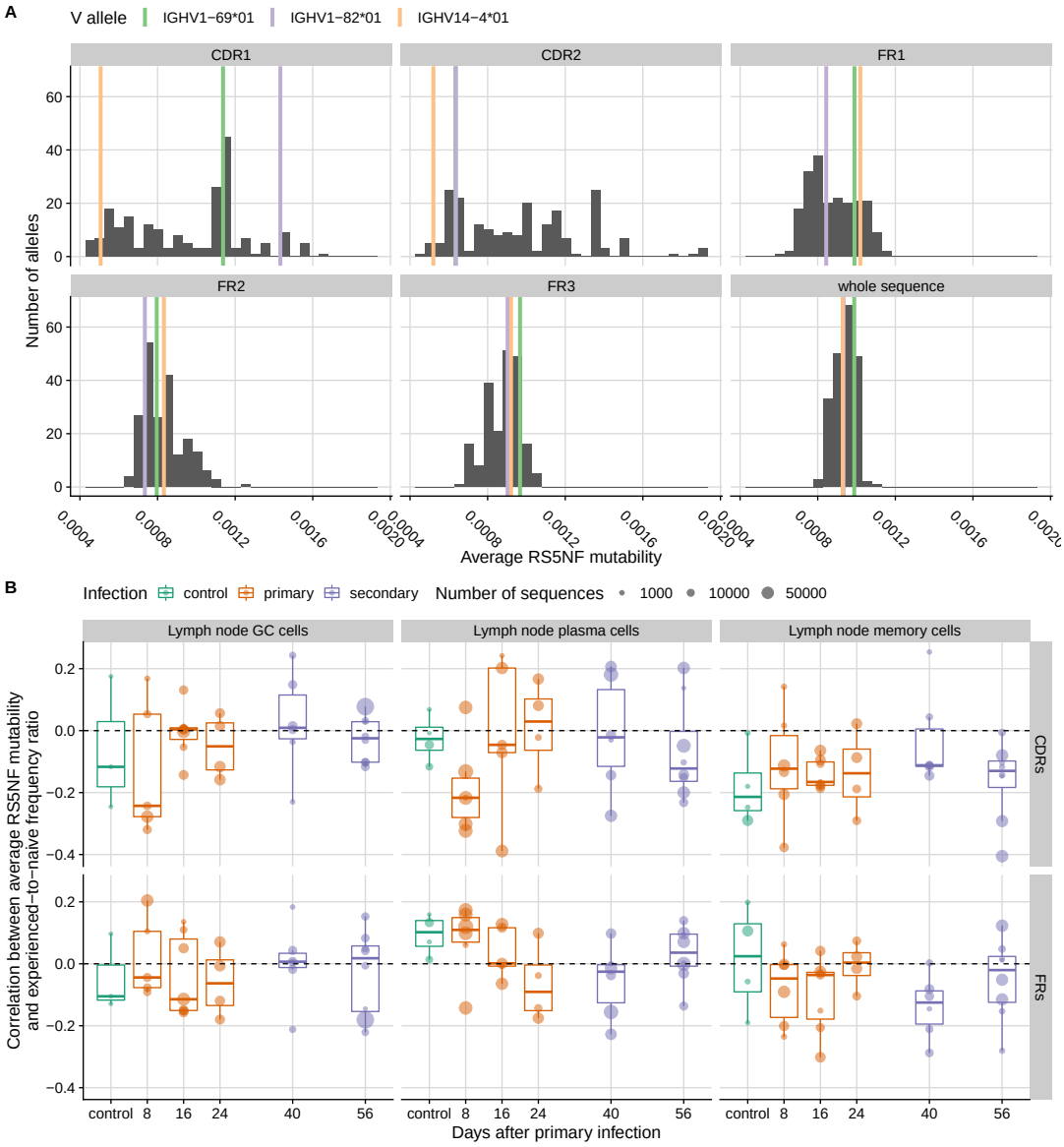

Figure 4–Figure supplement 6. Distribution of predicted mutability across V alleles (**A**), and correlations between predicted mutability and their frequency deviations from the naive repertoire (**B**). For each framework region (FR) and complementarity-determining region (CDR), we computed the average RS5NF mutability score from ***Cui et al. 2016*** across all 5-nucleotide motifs. In **B**, we computed an average across FRs weighed by the length of each FR, and similarly for CDRs. Each circle represents a mouse with at least 100 sequences each in the naive and experienced populations. Correlations were measured used Pearson's coefficient.

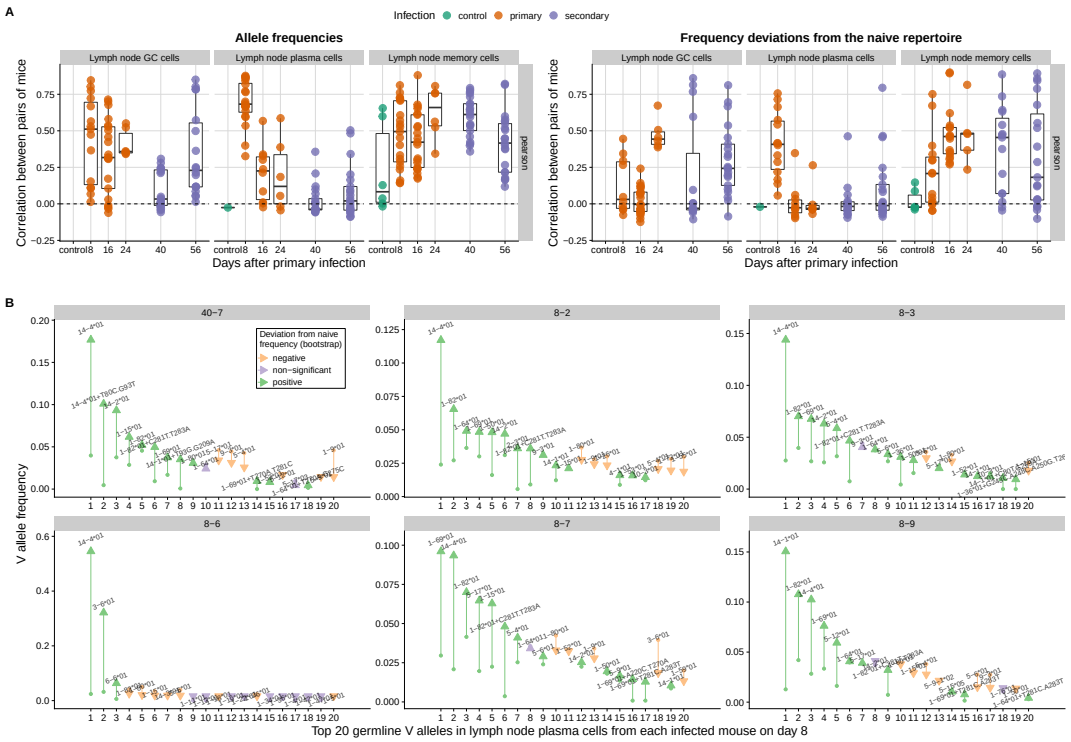

Figure 4–Figure supplement 7. Pairwise correlations between mice after collapsing identical reads from the same mouse, tissue, cell type and isotype. (**A**) Distribution of pairwise correlations at each time point. Each point represents a pair of mice with at least 100 reads each in the respective B cell population. We computed correlations using Pearson's coefficient and measured frequency deviations as the ratio between a V allele's frequency in an influenza-induced population and its frequency in the naive repertoire. (**B**) Frequency of the 20 most common V alleles in the lymph node plasma cells of each mouse 8 days after primary infection. Each panel represents an individual mouse. The arrows go from each allele's frequency in the naive repertoire to its frequency in lymph node plasma cells. Each allele was labelled as significantly over- or underrepresented in each mouse if the ratio of its experienced and naive frequencies was outside a 95% confidence interval obtained by bootstrap sampling ($n = 500$) of experienced frequencies from the naive repertoire (preserving the observed total number of sequences in each mouse). Mouse 40-7, which was sacrificed 8 days after the secondary infection, was considered a day-8 primary-infection mouse because it showed no signs of infection after the first inoculation and had ELISA titers similar to those of day-8 infected mice.

1010

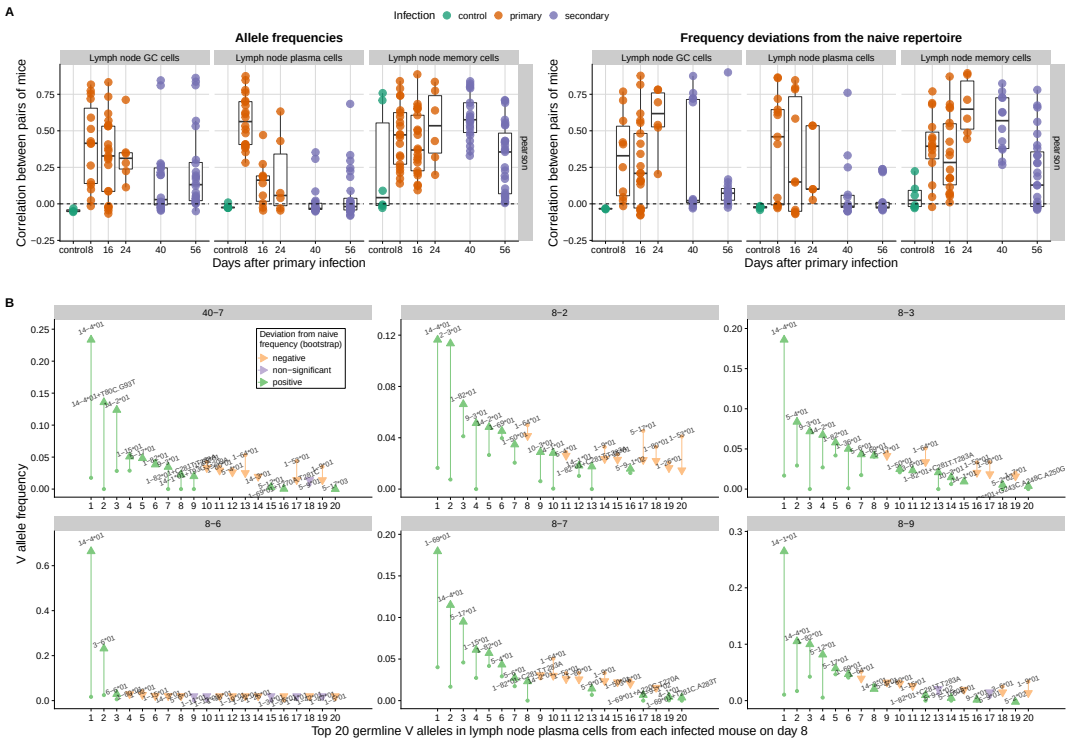

Figure 4–Figure supplement 8. Pairwise correlations between mice using an alternative dataset (***Greiff et al., 2017***) to estimate germline allele frequencies in the naive repertoire. (**A**) Distribution of pairwise correlations at each time point. Each point represents a pair of mice with at least 100 reads each in the respective B cell population. We computed correlations using Pearson's coefficient and measured frequency deviations as the ratio between a V allele's frequency in an influenza-induced population and its frequency in the naive repertoire. (**B**) Frequency of the 20 most common V alleles in the lymph node plasma cells of each mouse 8 days after primary infection. Each panel represents an individual mouse. The arrows go from each allele's frequency in the naive repertoire to its frequency in lymph node plasma cells. Each allele was labelled as significantly over- or underrepresented in each mouse if the ratio of its experienced and naive frequencies was outside a 95% confidence interval obtained by bootstrap sampling ($n = 500$) of experienced frequencies from the naive repertoire (preserving the observed total number of sequences in each mouse). Mouse 40-7, which was sacrificed 8 days after the secondary infection, was considered a day-8 primary-infection mouse because it showed no signs of infection after the first inoculation and had ELISA titers similar to those of day-8 infected mice.

1011